



Diploma Thesis

On the Visualization of Geometric Properties of Particular Spacetimes

Torsten Schönfeld

January 14, 2009

reviewed by

Prof. Dr. H.-H. von Borzeszkowski
Department of Theoretical Physics
Faculty II, Technische Universität Berlin

and

Priv.-Doz. Dr. M. Scherfner
Department of Mathematics
Faculty II, Technische Universität Berlin

Zusammenfassung auf Deutsch

Ziel und Aufgabenstellung dieser Diplomarbeit ist es, Möglichkeiten der Visualisierung in der Allgemeinen Relativitätstheorie zu finden. Das Hauptaugenmerk liegt dabei auf der Visualisierung geometrischer Eigenschaften einiger akausaler Raumzeiten, d.h. Raumzeiten, die geschlossene zeitartige Kurven erlauben.

Die benutzten und untersuchten Techniken umfassen neben den gängigen Möglichkeiten (Vektorfelder, Hyperflächen) vor allem das Darstellen von Geodäten und Lichtkegeln. Um den Einfluss der Raumzeitgeometrie auf das Verhalten von kräftefreien Teilchen zu untersuchen, werden in der Diplomarbeit mehrere Geodäten mit unterschiedlichen Anfangsbedingungen abgebildet. Dies erlaubt es zum Beispiel, die Bildung von Teilchenhorizonten oder Kaustiken zu analysieren. Die Darstellung von Lichtkegeln wiederum ermöglicht es, eine Vorstellung von der kausalen Struktur einer Raumzeit zu erlangen. Ein „Umkippen“ der Lichtkegel deutet beispielsweise oft auf signifikante Änderungen in der Raumzeit hin, z.B. auf die Möglichkeit von geschlossenen zeitartigen Kurven.

Zur Implementierung dieser Techniken wurde im Rahmen der Diplomarbeit ein MATHEMATICA-Paket namens GeodesicGeometry geschrieben, das die Anwendung der beschriebenen Visualisierungen auf beliebige Raumzeiten erlaubt. In der Arbeit werden die technischen Details zur numerischen Lösung der Geodätengleichungen und der Darstellung von Lichtkegeln erläutert.

Schließlich beschreibt die Arbeit die Anwendung dieser Techniken auf verschiedene Raumzeiten und die entsprechenden Resultate. Zunächst wird die Raumzeit von K. Gödel untersucht. Dabei werden verschiedene bekannte Erkenntnisse über die Struktur dieser interessanten Raumzeit graphisch dargestellt. Daran anschließend wird eine von M. Scherfner und M. Plaue entwickelte Erweiterung der Gödel-Raumzeit untersucht, die eine nichtverschwindende Expansion aufweist und damit realistischer ist. Ziel dabei ist vor allem die Darstellung des Einflusses der Expansion auf das Verhalten von Geodäten und auf die Bildung von geschlossenen zeitartigen Kurven. Den Abschluss bildet der Versuch, mittels der entwickelten Techniken eine Anschauung der verschiedenen von A. Ori vorgestellten „Zeitmaschinen“-Raumzeiten zu erlangen.

Die selbständige und eigenhändige Ausfertigung versichert an Eides statt

Unterschrift

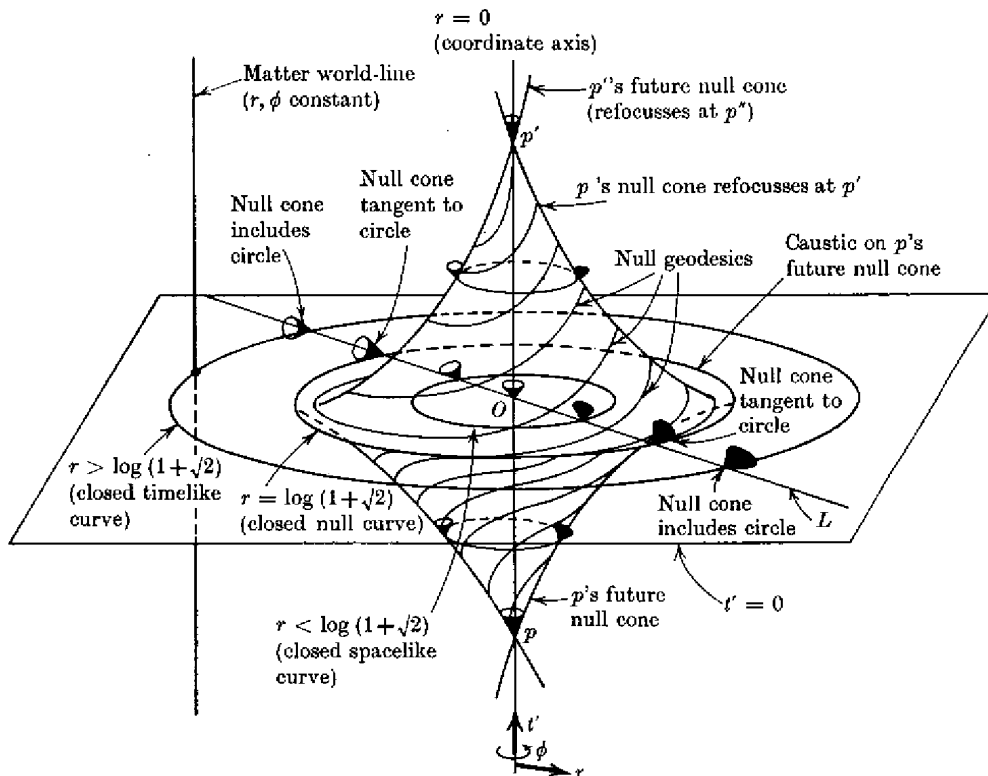
Berlin, den 14. Januar 2009

Contents

1	Preface	7
2	Differential Geometry	9
2.1	Semi-Riemannian Geometry	9
2.1.1	Manifolds and Maps	9
2.1.2	Tangent Spaces	10
2.1.3	Vector Bundles	11
2.1.4	Tensors	13
2.1.5	The Metric	15
2.1.6	The Levi-Civita Connection	16
2.1.7	Geodesics	19
2.1.8	The Lie Derivative and Killing Fields	22
2.2	Ricci Calculus	23
2.2.1	The Abstract Index Notation	23
2.2.2	Tensors and their Transformation	25
2.2.3	The Metric	27
2.2.4	The Derivatives	29
2.2.5	Geodesics and Killing Fields	32
3	General Relativity	35
3.1	Spacetime as a Lorentzian Manifold	35
3.2	The Field Equations	37
4	Visualization Techniques	41
4.1	The Role of Coordinates	41
4.2	Vector Fields and Hypersurfaces	42
4.3	Geodesics	44
4.4	Light Cones	47
5	Implementation	53
5.1	The Computer Algebra System Mathematica	53
5.2	The GeodesicGeometry Package	53
5.3	Solving the Geodesic Equations Numerically	54
5.4	Plotting Geodesics	55
5.5	Plotting Light Cones	56
6	Application to Particular Spacetimes	59
6.1	Gödel's Spacetime	59
6.2	Expanding Generalization of Gödel's Spacetime	65
6.3	Ori's Time-Machine Spacetimes	65

1 Preface

This diploma thesis deals with visualizing certain properties of spacetimes, particularly of acausal spacetimes. Inspiration and starting point for this are provided by a picture of the Gödel spacetime in Hawking and Ellis' book *The Large Scale Structure of Space-Time*:



The goal is to find possibilities to visualize other spacetimes in a similarly helpful way so as to aid understanding. Care was taken to make it easy to apply the developed techniques to arbitrary spacetimes.

To this end, the outline of this work is as follows. First, the necessary mathematical machinery is introduced and the physical background is explained. Then the used visualization techniques are described, including details of their implementation. Finally, these techniques are applied to particular acausal spacetimes.

Special thanks are due to Mike Scherfner for supervising the writing of this diploma thesis and to him and Matthias Plaue for answering all questions that came up.

2 Differential Geometry

This chapter introduces the mathematical preliminaries needed to understand those parts of spacetime geometry that are used in this diploma thesis. In particular, two very different yet related frameworks for studying spacetimes are detailed: semi-Riemannian geometry and the Ricci calculus.

Semi-Riemannian geometry is a generalization of the usual Euclidean geometry. Whereas Euclidean geometry deals with \mathbb{R}^n and objects embedded in it, semi-Riemannian geometry makes the geometric properties of certain entities, called manifolds, accessible without the need for them to be embedded in any \mathbb{R}^n . This is crucial for dealing with spacetime geometry.

Ricci calculus, on the other hand, is a set of rules for describing and, more importantly, for handling computations with spacetime quantities like the metric or curvature. It is very important for doing actual calculations—for finding the values of quantities or for solving differential equations, for example.

2.1 Semi-Riemannian Geometry

This section describes the basics of semi-Riemannian geometry. It starts by introducing the general theory of manifolds and then proceeds to semi-Riemannian manifolds and their properties. Finally, the attained mathematical machinery is employed to explain geodesics and a few quantities used to describe their behavior. The whole section is largely based on Pinkall and Peters (2006/2007) (which in turn is based on Hitchin (2003)) and Jänich (2005), and occasionally on Hawking and Ellis (1973).

2.1.1 Manifolds and Maps

An n -dimensional *differentiable manifold* is a paracompact Hausdorff space together with an associated *atlas* $\{(U_\alpha, \phi_\alpha)\}_\alpha$ consisting of *charts* (U_α, ϕ_α) which:

- cover the whole manifold: $\bigcup_\alpha U_\alpha = M$;
- map every chart neighborhood U_α homeomorphically to the open set $\phi_\alpha(U_\alpha) \subset \mathbb{R}^n$;
- and provide smooth *transition functions* $\phi_\beta \circ \phi_\alpha^{-1} : \phi_\alpha(U_\alpha \cap U_\beta) \rightarrow \phi_\beta(U_\alpha \cap U_\beta)$ between chart overlaps.

In the remainder, the term manifold will always mean a differentiable manifold.

A chart (U, ϕ) about a point $p \in M$ provides us with *coordinates* on a neighborhood of p . Since ϕ maps to \mathbb{R}^n , it can be written as $\phi = (\phi_1, \dots, \phi_n)$ where $\phi_i : M \rightarrow \mathbb{R}$ are the coordinate functions. For $p \in U$, the numbers $(\phi_1(p), \dots, \phi_n(p))$ denote the coordinates of p with respect to the chart (U, ϕ) .

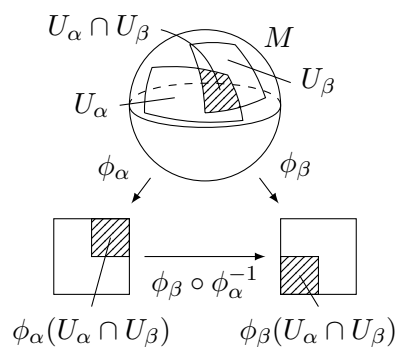


Figure 2.1: Part of an atlas $\{(U_\alpha, \phi_\alpha)\}$ on the manifold M . The transition function $\phi_\beta \circ \phi_\alpha^{-1}$ maps $\phi_\alpha(U_\alpha \cap U_\beta)$ smoothly to $\phi_\beta(U_\alpha \cap U_\beta)$.

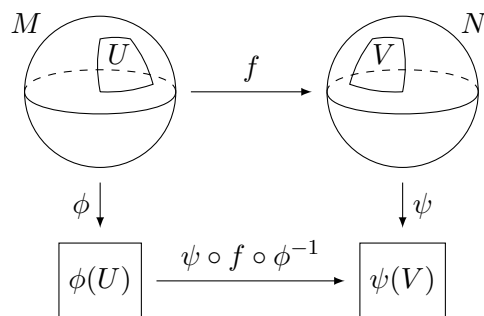


Figure 2.2: Map $f : M \rightarrow N$ between manifolds M and N and its pulled down variant. f is said to be smooth if the pulled down map $\psi \circ f \circ \phi^{-1}$ is smooth.

The definition of an atlas ensures that its charts overlap in a smooth way, i.e. that the change from one chart to another is always smooth. See figure 2.1 for an illustration of part of an atlas and the corresponding transition function.

A set $O \subset M$ is said to be **open** if for all charts (U, ϕ) of an atlas for M , the set $\phi(O \cap U) \subset \mathbb{R}^n$ is open. A map $f : M \rightarrow N$ between M and another manifold N is said to be **continuous** if for all open sets $A \subset N$ the preimage $f^{-1}(A) \subset M$ is open. A map $f : M \rightarrow N$ is said to be **smooth** at $p \in M$ if for a chart (U, ϕ) about p and a chart (V, ψ) about $f(p)$ the function $\psi \circ f \circ \phi^{-1} : \phi(U) \rightarrow \psi(V)$ is smooth. Notation: $C^\infty(M, N) := \{f : M \rightarrow N \mid f \text{ smooth}\}$ and $C^\infty(M) := C^\infty(M, \mathbb{R})$. For an illustration of these definitions, see figure 2.2.

On first sight, the definition of smoothness might seem to depend on the chosen chart in areas where two charts overlap. But the pulled down map in one chart will only differ from the pulled down map in another chart by the prepended transition function, which is defined to be smooth. So the concept does not depend on the chosen chart.

2.1.2 Tangent Spaces

Now that we have smooth maps on manifolds, we would also like to be able to differentiate them, i.e. approximate them with linear ones. The obvious idea of using the differential $d_x(\psi \circ f \circ \phi^{-1})$ of the pulled down map turns out to be unusable: it depends on the chosen charts. Instead, we will linearly approximate the manifolds themselves at every point with vector spaces $T_p M$ called tangent spaces. The differential will then be a linear map $d_p f : T_p M \rightarrow T_{f(p)} N$ between the tangent spaces. There are multiple equivalent ways to define the tangent space. We will use one of them here, and introduce another one in section 2.2.

A **tangent vector** at p is a derivation, i.e. a linear map $v : C^\infty(M) \rightarrow \mathbb{R}$ which satisfies the Leibniz rule $v(\lambda \cdot \mu) = v(\lambda) \cdot \mu + \lambda \cdot v(\mu)$ for all $\lambda, \mu \in C^\infty(M)$. The **tangent space** $T_p M$ is the vector space of all tangent vectors at p .

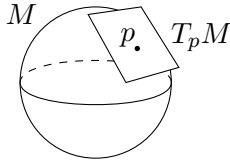


Figure 2.3: The tangent space $T_p M$ at the manifold M is a vector space that linearly approximates M at p .

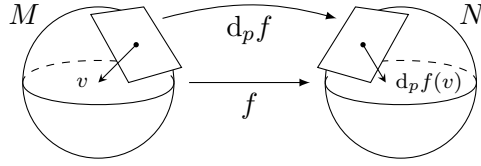


Figure 2.4: The differential $d_p f$ of a map $f : M \rightarrow N$ maps vectors in $T_p M$ to vectors in $T_{f(p)} N$.

For a map $f \in C^\infty(M, N)$ the **differential** $d_p f$ at $p \in M$ is the map $d_p f : T_p M \rightarrow T_{f(p)} N$, $v \mapsto v \circ f^*$, where the **pullback function** f^* is defined by $f^* \lambda = \lambda \circ f$ for all $\lambda \in C^\infty(N)$. That is, the tangent vector $d_p f(v)$ acts on a $\lambda \in C^\infty(N)$ as

$$(d_p f(v))(\lambda) = v(\lambda \circ f).$$

See figures 2.3 and 2.4 for illustrations.

As can be seen easily, the differential of the identity map is the identity map on the tangent space: $d_p \text{id} = \text{id}_{T_p M}$. A bit more involved but still easy to show is that the differential satisfies the chain rule: $d_p(g \circ f) = d_{f(p)} g \circ d_p f$ for all $f \in C^\infty(M_1, M_2)$, $g \in C^\infty(M_2, M_3)$. These two relations provide an indication that the above definition of a differential actually makes sense.

When we choose a chart (U, ϕ) about $p \in M$, the coordinate functions $\{\phi_i\}$ induce a set of tangent vectors $\{\partial_i^p\}$ in $T_p M$:

$$\partial_i^p \lambda := \frac{\partial(\lambda \circ \phi^{-1})}{\partial \phi_i}(\phi(p)) \quad \text{for every } \lambda \in C^\infty(M).$$

That is, ∂_i^p acts on a map λ by differentiating its coordinate representation $\lambda \circ \phi^{-1}$ with respect to the i -th coordinate ϕ_i . It can be shown¹ that the n **coordinate vectors** $\{\partial_i^p\}$ constitute a basis of $T_p M$ called the **canonical basis** with respect to the chart (U, ϕ) . Every tangent vector $v \in T_p M$ can then be written as

$$v = \sum_{i=1}^n v_i \partial_i^p \quad \text{with } v_i = v \phi_i.$$

Thus, we see that the tangent spaces of an n -dimensional manifold are n -dimensional as well.

2.1.3 Vector Bundles

We now have vectors and differentials defined at points of manifolds. Often, it is useful to have structures that are defined globally, on the whole manifold. We will define these new structures in the framework of vector bundles. A **vector bundle** of rank n over M

¹See Lovelock and Rund (1975, pages 332ff) for a proof.

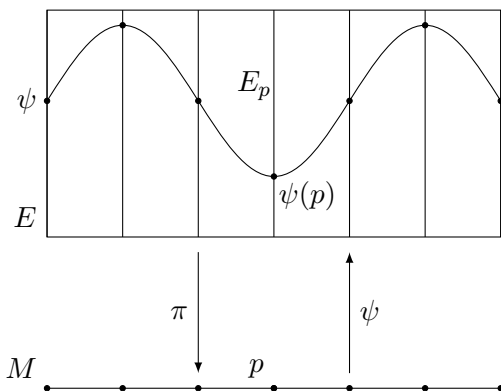


Figure 2.5: A vector bundle E over the manifold M is a manifold which assigns to each point $p \in M$ the fibre E_p . The projection map π maps each fibre E_p to its base point p . A cross section $\psi \in \Gamma(E)$ maps to each point $p \in M$ a vector in E_p .

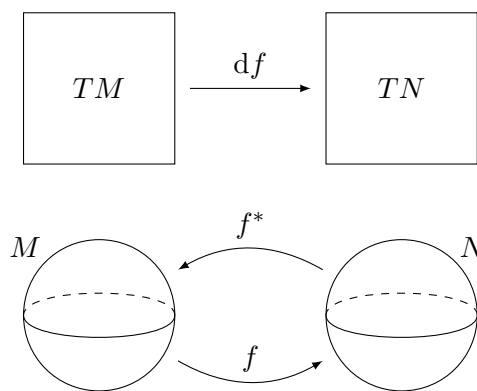


Figure 2.6: The map $f : M \rightarrow N$ and its related maps $f^* : C^\infty(N) \rightarrow C^\infty(M)$ and $df : TM \rightarrow TN$. f^* maps functions defined on N to functions defined on M . df maps tangent vectors at $p \in M$ to tangent vectors at $f(p) \in N$.

is a tuple (E, π) of a manifold E and a smooth projection map $\pi : E \rightarrow M$ such that the following holds:

1. For every point $p \in M$ there is a **bundle chart**, i.e. a neighborhood $U_\alpha \subset M$ containing p and a smooth map $\Phi_\alpha : \pi^{-1}(U_\alpha) \rightarrow U_\alpha \times \mathbb{R}^n$ such that Φ_α maps the **fibre** $E_q := \pi^{-1}(q)$ to the vector space $\{q\} \times \mathbb{R}^n$ for every $q \in U_\alpha$. Thus, $\pi^{-1}(p)$ has the structure of an n -dimensional vector space for every $p \in M$.
2. For $U_\alpha, U_\beta \subset M$ the transition function $\Phi_\alpha \circ \Phi_\beta^{-1}$ is of the form

$$\begin{aligned} \Phi_\alpha \circ \Phi_\beta^{-1} : (U_\alpha \cap U_\beta) \times \mathbb{R}^n &\rightarrow (U_\alpha \cap U_\beta) \times \mathbb{R}^n \\ (p, v) &\mapsto (p, G_{\alpha\beta}(p)v), \end{aligned}$$

where $G_{\alpha\beta} : U_\alpha \cap U_\beta \rightarrow \text{GL}(n, \mathbb{R})$ is smooth. That is, in areas where bundle charts overlap, vectors that belong to the same point only differ by a linear and invertible transformation.

A **cross section** of a vector bundle E is a smooth map $\psi : M \rightarrow E$ such that $\pi \circ \psi = \text{id}_M$. The set of all cross sections of E form the vector space $\Gamma(E)$.

Intuitively speaking, a vector bundle over a manifold assigns to each point of the manifold a real vector space in such a way that the vector spaces of different points do not overlap. A cross section then assigns to every point of the manifold a vector in the corresponding vector space of the vector bundle. These cross sections will provide the global structures we seek. For an illustration of these concepts, see figure 2.5 and the following two examples.

Example 1: Consider the **trivial bundle** $E = M \times \mathbb{R}^n$. The projection map π is simply $(p, v) \mapsto p$ for $p \in M$ and $v \in \mathbb{R}^n$, and a bundle chart is given by (E, id_E) .

On this vector bundle, every smooth map $f : M \rightarrow \mathbb{R}^n$ defines a cross section $\psi : M \rightarrow E$, $\psi(p) = (p, f(p))$.

Example 2: The *tangent bundle* $E = TM := \bigcup_{p \in M} T_p M$ is perhaps the most important vector bundle. The projection map π uses the tangent vectors' "knowledge" (which we usually suppress in the notation) of the point on the manifold they are attached to: $\pi(v_p) = p$ for $v_p \in T_p M$. The bundle atlas $\{(U_\alpha, \Phi_\alpha)\}$ is constructed from the atlas $\{(U_\alpha, \phi_\alpha)\}$ of M by

$$\Phi_\alpha(v_p) = \left(p, \left(v_p(\phi_\alpha^{(1)}), \dots, v_p(\phi_\alpha^{(n)}) \right) \right) \quad \text{for every } v_p \in \pi^{-1}(U_\alpha) = T_{U_\alpha} M.$$

To see that item 2 of the definition of a vector bundle is fulfilled, let $p \in M$, $v_p \in T_p M$ and let (U_α, ϕ_α) and (U_β, ϕ_β) both be charts about p . Then one can show that the coordinate representations of v_p obey the following relation²:

$$\left(v_p(\phi_\alpha^{(1)}), \dots, v_p(\phi_\alpha^{(n)}) \right) = d_{\phi_\beta(p)}(\phi_\alpha \circ \phi_\beta^{-1}) \cdot \left(v_p(\phi_\beta^{(1)}), \dots, v_p(\phi_\beta^{(n)}) \right).$$

Thus we have

$$\Phi_\alpha \circ \Phi_\beta^{-1}(p, v_p) = \left(p, d_{\phi_\beta(p)}(\phi_\alpha \circ \phi_\beta^{-1}) \cdot v_p \right),$$

which satisfies the definition. A cross section $\psi \in \Gamma(TM)$ of TM is called *vector field*. To each point $p \in M$, it maps a vector $v \in T_p M$. Additionally, ψ can also be interpreted as $\psi : C^\infty(M) \rightarrow C^\infty(M)$, $f \mapsto \psi f$ with $(\psi f)(p) := (\psi(p))(f)$. The Leibniz rule holds for ψ then: $\psi(f \cdot g) = (\psi f) \cdot g + f \cdot (\psi g)$. All this enables us to define the *differential* of a map $f : M \rightarrow N$ globally: $df : TM \rightarrow TN$, $\psi \mapsto df(\psi)$ with $(df(\psi))(p) := d_p f(\psi(p))$. See figure 2.6 for an illustration of the maps df and f^* .

Just like for tangent vectors, a chart (U, ϕ) also induces a *bundle basis* $\{\partial_i\}$ for vector fields:

$$\partial_i \lambda := \frac{\partial(\lambda \circ \phi^{-1})}{\partial \phi_i} \circ \phi \quad \text{for every } \lambda \in C^\infty(M).$$

Every $\psi \in \Gamma(TM)$ can thus be written as

$$\psi = \sum_{i=1}^n \psi_i \partial_i \quad \text{with } \psi_i = \psi \phi_i.$$

2.1.4 Tensors

To conclude the discussion of general manifolds, we introduce the concept of tensors on manifolds. We will do this in multiple steps. First, we define the vector space of multilinear forms on tangent vectors. The union of all these vector spaces will form a vector bundle. Then, we introduce differential forms as cross sections on this vector

²For a proof, see Jänich (2005, pages 33ff).

bundle. Finally, tensors are defined as those multilinear maps on vector fields which are built from a differential form.

A **multilinear k -form** ω_p at $p \in M$ on a vector bundle E over M is a map

$$\omega_p : \underbrace{T_p M \times \cdots \times T_p M}_k \rightarrow E_p$$

which satisfies

$$\begin{aligned} \omega_p(v_1, \dots, \rho(v_j + w_j), \dots, v_k) &= \rho \omega_p(v_1, \dots, v_j, \dots, v_k) \\ &\quad + \rho \omega_p(v_1, \dots, w_j, \dots, v_k) \end{aligned}$$

for all $\rho \in \mathbb{R}$ and $v_1, \dots, v_k, w_j \in T_p M$. The vector space of all these multilinear k -forms is called $\mathcal{J}^k(T_p M)$. The union $\mathcal{J}^k(TM) := \bigcup_{p \in M} \mathcal{J}^k(T_p M)$ forms a vector bundle over M . A **differential k -form** over M is a cross section $\omega \in \Omega^k(M) := \Gamma(\mathcal{J}^k(TM))$, i.e. a map which assigns to every $p \in M$ a multilinear k -form $\omega_p \in \mathcal{J}^k(T_p M)$.

A multilinear map

$$\tilde{\omega} : \underbrace{\Gamma(TM) \times \cdots \times \Gamma(TM)}_k \rightarrow \Gamma(E)$$

is called a **tensor** of rank k if there is an $\omega \in \Omega^k(M)$ with

$$(\tilde{\omega}(\psi_1, \dots, \psi_k))(p) = (\omega(p))(\psi_1(p), \dots, \psi_k(p))$$

for all $\psi_1, \dots, \psi_k \in \Gamma(TM)$.

In other words, a tensor is a map which takes k vector fields ψ_1, \dots, ψ_k and yields a cross section whose value at $p \in M$ only depends on the values of ψ_1, \dots, ψ_k at p . The following theorem provides a more convenient criterion to test if a given map is a tensor.

Theorem 1: Let M be a manifold and E a vector bundle over M . A multilinear map $\tilde{\omega} : \Gamma(TM) \times \cdots \times \Gamma(TM) \rightarrow \Gamma(E)$ is a tensor if and only if

$$\tilde{\omega}(\psi_1, \dots, \lambda\psi_j, \dots, \psi_k) = \lambda\tilde{\omega}(\psi_1, \dots, \psi_k)$$

for all $\lambda \in C^\infty(M)$ and $\psi_1, \dots, \psi_k \in \Gamma(TM)$. In other words: $\tilde{\omega}$ is a tensor if and only if it is $C^\infty(M)$ -**linear**.

Proof. \Rightarrow : Let $\tilde{\omega}$ be a tensor. Then there is an $\omega \in \Omega^k(M)$ with

$$\begin{aligned} (\tilde{\omega}(\psi_1, \dots, \lambda\psi_j, \dots, \psi_k))(p) &= (\omega(p))(\psi_1(p), \dots, \lambda(p)\psi_j(p), \dots, \psi_k(p)) \\ &= \lambda(p)(\omega(p))(\psi_1(p), \dots, \psi_k(p)) \\ &= \lambda(p)(\tilde{\omega}(\psi_1, \dots, \psi_k))(p). \end{aligned}$$

\Leftarrow : For $p \in M$ choose a chart (U, ϕ) about p . Without loss of generality, we can confine ourselves to U . Let $\{\partial_i\}$ be the canonical basis field of TM induced by (U, ϕ) . We can then express every $\psi_j \in \Gamma(TM)$ as

$$\psi_j = \sum_i \psi_{ji} \partial_i \quad \text{with } \psi_{ji} \in C^\infty(M).$$

Now define $\omega \in \Omega^k(M)$ by

$$(\omega(p))(\partial_{i_1}(p), \dots, \partial_{i_k}(p)) = (\tilde{\omega}(\partial_{i_1}, \dots, \partial_{i_k}))(p).$$

Then we have

$$\begin{aligned} (\tilde{\omega}(\psi_1, \dots, \psi_k))(p) &= \sum_{i_1, \dots, i_k} \psi_{1i_1}(p) \cdots \psi_{ki_k}(p) (\tilde{\omega}(\partial_{i_1}, \dots, \partial_{i_k}))(p) \\ &= \sum_{i_1, \dots, i_k} \psi_{1i_1}(p) \cdots \psi_{ki_k}(p) (\omega(p))(\partial_{i_1}(p), \dots, \partial_{i_k}(p)) \\ &= (\omega(p))(\psi_1(p), \dots, \psi_k(p)). \end{aligned}$$

□

2.1.5 The Metric

Now that we know what tangent vectors are, we would like to be able to measure some of their properties. It will also be useful to know how a given vector field varies in the direction of another vector field. This and the next section introduce the concepts necessary for the above and describes some important new structures arising from these concepts. We start with the metric.

A **semi-Riemannian metric** on a manifold M is a map $g : \Gamma(TM) \times \Gamma(TM) \rightarrow C^\infty(M)$ where

$$(g(\psi, \chi))(p) := g_p(\psi(p), \chi(p))$$

is smooth for all $p \in M$ and $\psi, \chi \in \Gamma(TM)$ and where $g_p(\cdot, \cdot)$ is a non-degenerate symmetric and possibly indefinite scalar product in T_pM . A tuple (M, g) is called a **semi-Riemannian manifold** if M is a manifold and g is a semi-Riemannian metric on M .

So a semi-Riemannian metric g assigns to two vector fields a smooth map. This map in turn assigns to every point on the manifold the scalar product of the values of the vector fields at this point. Since $C^\infty(M)$ can be thought of as the space of cross sections on the trivial bundle $M \times \mathbb{R}$, g is actually a tensor with $g(\cdot, \cdot) \in \Omega^2(M)$ as the corresponding differential form. The length of a vector $v \in T_pM$ is then simply defined as $\|v\| = \sqrt{g_p(v, v)}$.

The type of a metric g can be succinctly summarized by what is called its **signature**. This is a tuple of plus and minus signs denoting the signs of the eigenvalues of the metric. By a suitable choice of coordinates, g can at any point of the manifold be brought into the form $\text{diag}(\lambda_1, \dots, \lambda_n)$ with $\lambda_i = \pm 1$. This form makes it easy to read off the signature. There are two basic types that are interesting. In what is called the **Riemannian case**, g is positive definite and its signature therefore is $(+, \dots, +)$.

In the **Lorentzian case**, g has signature $(+, -, -, -)^3$ which means that g is indefinite, i.e. for any tangent vector $v \in T_pM$ its length as measured by g_p might be negative, null,

³Or $(-, +, +, +)$ depending on personal preferences. The two choices are basically equivalent except for annoying sign differences in various expressions.

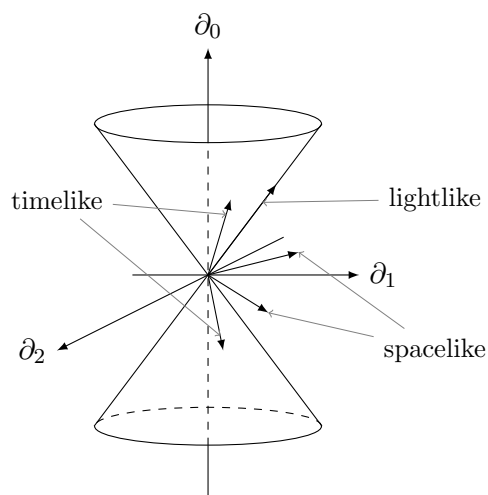


Figure 2.7: The three types of tangent vectors in the coordinate system $\{\partial_0, \partial_1, \partial_2\}$. The coordinate ∂_3 has been suppressed. Timelike vectors lie inside the light cones spanned by lightlike vectors. Spacelike vectors lie outside the light cones.

or positive. These three possibilities are used to classify the vectors in every tangent space T_pM :

$$v \in T_pM \text{ is called } \begin{cases} \text{spacelike} & \text{if } g_p(v, v) < 0, \\ \text{lightlike} & \text{if } g_p(v, v) = 0, \\ \text{timelike} & \text{if } g_p(v, v) > 0. \end{cases}$$

When we choose the basis $\{\partial_\mu\}$ of T_pM that brings g into the form $\text{diag}(+1, -1, -1, -1)$, $g_p(v, v)$ can be expressed in terms of the projections of v onto $\{\partial_\mu\}$:

$$g_p(v, v) = \langle v, \partial_0 \rangle - \langle v, \partial_1 \rangle - \langle v, \partial_2 \rangle - \langle v, \partial_3 \rangle.$$

So we see that v is spacelike, lightlike, or timelike if the component $\langle v, \partial_0 \rangle$ is, respectively, smaller than, equal to, or bigger than the sum of the other components. The lightlike vectors form cones in the tangent space which separate timelike from spacelike vectors. See figure 2.7 for an illustration. As we will see later, Lorentzian manifolds are the ones that are used to model spacetime.

2.1.6 The Levi-Civita Connection

The next item on the wish list is a directional derivative for vector fields, or more generically for cross sections. It is instructional to first consider how this might be defined on known ground.

Example 3: Let M be a manifold and let $E = M \times \mathbb{R}$ be the trivial bundle. Let $v \in \Gamma(TM)$ and $\psi \in \Gamma(E)$ and let $\lambda \in C^\infty(M)$ be the generator of ψ , i.e. $\psi(p) = (p, \lambda(p))$. How would the directional derivative $\nabla_v \psi$ of ψ in the direction

v look like? We would like it to yield a new cross section, so $\nabla_v \psi \in \Gamma(E)$. One natural definition would then be the following:

$$(\nabla_v \psi)(p) := \left(p, (v(p))(\lambda) \right).$$

That is, we use $v(p) \in T_p M$ to differentiate λ . For $\mu \in C^\infty(M)$, this definition satisfies the following rules:

$$\begin{aligned} \nabla_{\mu v} \psi &= \mu \nabla_v \psi, \\ \nabla_v(\mu \psi) &= \mu \nabla_v \psi + v(\mu) \psi. \end{aligned}$$

Additionally we have

$$\begin{aligned} \nabla_{[v,w]} \psi &= \nabla_{vw - wv} \psi \\ &= (\cdot, (vw - wv)(\lambda)) \\ &= (\cdot, v(w(\lambda))) - (\cdot, w(v(\lambda))) \\ &= \nabla_v(\cdot, w(\lambda)) - \nabla_w(\cdot, v(\lambda)) \\ &= \nabla_v(\nabla_w \psi) - \nabla_w(\nabla_v \psi). \end{aligned} \tag{2.1}$$

With the motivation provided by this example, we define a **connection** on the vector bundle E over the manifold M as a linear map $\nabla : \Gamma(TM) \times \Gamma(E) \rightarrow \Gamma(E)$ such that for all $v \in \Gamma(TM)$, $\psi \in \Gamma(E)$, and $\lambda \in C^\infty(M)$ the following holds:

1. $\nabla_{\lambda v} \psi = \lambda \nabla_v \psi$,
2. $\nabla_v(\lambda \psi) = \lambda \nabla_v \psi + v(\lambda) \psi$.

An **affine connection** on M is a connection on TM . The **curvature tensor** of ∇ is the map

$$\begin{aligned} R : \Gamma(TM) \times \Gamma(TM) \times \Gamma(E) &\rightarrow \Gamma(E) \\ R(v, w) \psi &= \nabla_v(\nabla_w \psi) - \nabla_w(\nabla_v \psi) - \nabla_{[v,w]} \psi. \end{aligned} \tag{2.2}$$

∇ is said to be **flat** if $R(v, w) \psi = 0$ for all $v, w \in \Gamma(TM)$, $\psi \in \Gamma(E)$. Note that, due to (2.1), the expression (2.2) vanishes for the previous example, so the connection described there is flat. The **torsion tensor** T of ∇ is the map

$$\begin{aligned} T : \Gamma(TM) \times \Gamma(TM) &\rightarrow \Gamma(TM) \\ T(v, w) &= \nabla_v w - \nabla_w v - [v, w]. \end{aligned}$$

∇ is said to be **torsion-free** if $T(v, w) = 0$ for all $v, w \in \Gamma(TM)$. It is easy to show that the curvature and the torsion tensor are actually tensors by using theorem 1.

An affine connection ∇ on M is said to be **metric preserving** or just **metric** for the semi-Riemannian metric g on M if for all $u, v, w \in \Gamma(TM)$ the following holds:

$$u(g(v, w)) = g(\nabla_u v, w) + g(v, \nabla_u w).$$

Now it turns out that there is exactly one torsion-free metric affine connection on every semi-Riemannian manifold. This is sometimes called the fundamental theorem of semi-Riemannian geometry.

Theorem 2: Let (M, g) be a semi-Riemannian manifold. Then there is exactly one torsion-free metric affine connection ∇ on M . ∇ is called the **Levi-Civita connection** of (M, g) .

Proof. Uniqueness: Let ∇ be an affine connection on M that is torsion-free and metric. Let $u, v, w \in \Gamma(TM)$. Then we have:

$$u(g(v, w)) = g(\nabla_u v, w) + g(v, \nabla_u w) \quad (2.3)$$

$$v(g(w, u)) = g(\nabla_v w, u) + g(w, \nabla_v u) \quad (2.4)$$

$$w(g(u, v)) = g(\nabla_w u, v) + g(u, \nabla_w v). \quad (2.5)$$

Forming (2.3) + (2.4) - (2.5) we get:

$$\begin{aligned} & u(g(v, w)) + v(g(w, u)) - w(g(u, v)) \\ &= g(\nabla_u v + \nabla_v u, w) + g(\nabla_u w - \nabla_w u, v) + g(\nabla_v w - \nabla_w v, u) \\ &= g(\nabla_u v + \nabla_v u - [u, v], w) + g([u, w], v) + g([v, w], u). \end{aligned}$$

Thus, $\nabla_u v$ is determined by the **Koszul formula**:

$$\begin{aligned} 2g(\nabla_u v, w) &= u(g(v, w)) + v(g(w, u)) - w(g(u, v)) \\ &\quad + g([u, v], w) - g([u, w], v) - g([v, w], u). \end{aligned} \quad (2.6)$$

Existence: Let $u, v \in \Gamma(TM)$. Define $\nabla_u v$ by (2.6). Then we need to show that this ∇ is a torsion-free metric connection.

- Making use of the tensorial character of g , of the Leibniz rule for vector fields, and of $[\lambda u, v] = \lambda[u, v] - (v\lambda)u$, we can show:

$$\begin{aligned} g(\nabla_{\lambda u} v, w) &= g(\lambda \nabla_u v, w), \\ g(\nabla_u(\lambda v), w) &= g(\lambda \nabla_u v, w) + g((u\lambda)v, w). \end{aligned}$$

Thus ∇ is a connection.

- We have $g(\nabla_u v, w) - g(\nabla_v u, w) = g([u, v], w)$, so ∇ is torsion-free.
- Finally, we have $g(\nabla_u v, w) + g(\nabla_u w, v) = ug(v, w)$, so ∇ is metric.

□

The curvature tensor R of the Levi-Civita connection satisfies what are called the **symmetries of the curvature tensor** which we note here without proof:

1. $0 = R(u, v)w + R(w, u)v + R(u, w)v$,
2. $R(u, v)w = -R(v, u)w$,
3. $g(R(u, v)w, t) = -g(R(u, v)t, w)$,
4. $g(R(u, v)w, t) = g(R(v, u)t, w)$,

for all $t, u, v, w \in \Gamma(TM)$.

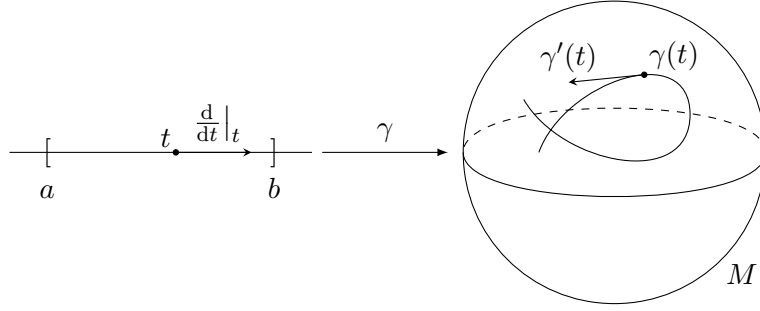


Figure 2.8: A curve $\gamma : [a, b] \rightarrow M$ on the manifold M , and its derivative γ' . The latter is a vector field which assigns to every $t \in [a, b]$ a tangent vector $\gamma'(t) \in T_{\gamma(t)}M$.

2.1.7 Geodesics

A **curve** on a manifold M is a smooth map $\gamma : [a, b] \rightarrow M$ with $a, b \in \mathbb{R}$. The **derivative** $\gamma' \in \Gamma(TM)$ of γ is given by $\gamma' = d\gamma(d/dt)$. That is, for $t \in [a, b]$, the tangent vector $\gamma'(t) \in T_{\gamma(t)}M$ acts on $f \in C^\infty(M)$ as:

$$(\gamma'(t))(f) = \left(d_t \gamma \left(\frac{d}{dt} \Big|_t \right) \right) (f) = \frac{d}{dt} \Big|_t (f \circ \gamma).$$

See figure 2.8 for an illustration of a curve and its derivative.

The derivative γ' is an example of the more general notion of a **vector field v along γ** , defined as a smooth map $v : [a, b] \rightarrow TM$ with $v(t) \in T_{\gamma(t)}M$. Given a vector field $\psi \in \Gamma(TM)$, a curve $\gamma : [a, b] \rightarrow M$ is called **integral curve of ψ** if $\gamma'(t) = \psi(\gamma(t))$ for all $t \in [a, b]$. Finally, given a semi-Riemannian manifold (M, g) and its Levi-Civita connection ∇ , $\gamma : [a, b] \rightarrow M$ is called a **geodesic** if $\gamma'' := \nabla_{\gamma'} \gamma' = 0$.

Note that “ $\nabla_{\gamma'} \gamma'$ ” is just a heuristic, and technically not completely correct. ∇ can only operate on vector fields that are defined globally, but γ' is defined only on $\{\gamma(t) \mid t \in [a, b]\}$. This incompatibility can be worked around with some effort.⁴ This effort does not provide any new insight, however. The intuition provided by “ $\nabla_{\gamma'} \gamma'$ ” as the acceleration of γ is good enough. As an indication for this, we can show that a geodesic γ has constant velocity:

$$\frac{d}{dt} \|\gamma'(t)\| = \frac{d}{dt} g_{\gamma(t)}(\gamma'(t), \gamma'(t)) = 2g_{\gamma(t)}(\gamma''(t), \gamma'(t)) = 0.$$

In \mathbb{R}^2 , the length $L(\gamma)$ of a curve $\gamma : [a, b] \rightarrow \mathbb{R}^2$, $\gamma(t) = (x(t), y(t))$ is derived from the distance formula $d = \sqrt{\Delta x^2 + \Delta y^2}$ by taking the limit $\Delta x \rightarrow dx$ and integrating:

$$L(\gamma) = \int_a^b \sqrt{dx^2 + dy^2} = \int_a^b \sqrt{\left(\frac{dx}{dt}\right)^2 + \left(\frac{dy}{dt}\right)^2} dt = \int_a^b \sqrt{\langle \gamma'(t), \gamma'(t) \rangle} dt.$$

Thus, on a semi-Riemannian manifold (M, g) we define the **length $L(\gamma)$ of a curve**

⁴See Gallot, Hulin, and Lafontaine (2004, pages 75ff.) for example.

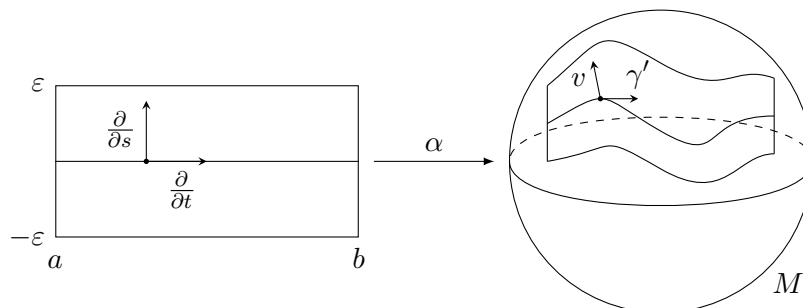


Figure 2.9: A variation $\alpha : (-\varepsilon, \varepsilon) \times [a, b] \rightarrow M$ of the curve $\gamma : [a, b] \rightarrow M$ and its variation vector field v . The latter is a vector field along γ which “points” to the neighboring curve of the variation.

$\gamma : [a, b] \rightarrow M$ by

$$L(\gamma) = \int_a^b \sqrt{g_{\gamma(t)}(\gamma'(t), \gamma'(t))} dt.$$

Note that when the metric is indefinite, as in the Lorentzian case, this notion of length can be misleading: a curve whose tangent vectors are lightlike always has zero length. For simplicity, we will concentrate in the following on timelike curves or, equivalently, on metrics with Riemannian signature. For details on how to deal with the Lorentzian case, see Hawking and Ellis (1973, pages 102ff.) or O’Neill (1983, pages 288ff.).

The definition of length is independent of the choice of parametrization of γ , as can be shown easily with the usual substitution rule. So when a curve has constant non-zero velocity, this allows us to reparametrize it so that $\|\gamma'\| = 1$, i.e. we can assume that such a curve is parametrized by arc length.

To show that geodesics are curves with extremal length, we need to look at variations of curves. A **variation of** γ is a smooth map $\alpha : (-\varepsilon, \varepsilon) \times [a, b] \rightarrow M$ with $\alpha(0, t) = \gamma(t)$ for all $t \in [a, b]$. Notation: $\gamma_s(t) := \alpha(s, t)$, so $\gamma_0 = \gamma$. The vector field defined by

$$v(t) = \left. \frac{\partial \alpha(s, t)}{\partial s} \right|_{s=0} = d_{(s,t)} \alpha \left(\left. \frac{\partial}{\partial s} \right) \right|_{s=0} \in T_{\gamma(t)} M$$

is called **variation vector field of** α . See figure 2.9 for an illustration of this concept.

Theorem 3: Let (M, g) be a semi-Riemannian manifold, ∇ its Levi-Civita connection, $\gamma : [a, b] \rightarrow M$ a curve with $\|\gamma'\| = 1$, $\alpha : (-\varepsilon, \varepsilon) \times [a, b] \rightarrow M$ a variation of γ , and $v \in \Gamma(TM)$ the variation vector field of α . Then:

$$\left. \frac{dL(\gamma_s)}{ds} \right|_{s=0} = g_{\gamma(\cdot)}(v(\cdot), \gamma'(\cdot)) \Big|_a^b - \int_a^b g_{\gamma(t)}(v(t), \gamma''(t)) dt.$$

Proof. For ease of notation, we will use $\langle v, \gamma' \rangle := g_{\gamma(\cdot)}(v(\cdot), \gamma'(\cdot))$. With this, the assertion reads

$$\left. \frac{dL(\gamma_s)}{ds} \right|_{s=0} = \langle v, \gamma' \rangle \Big|_a^b - \int_a^b \langle v, \gamma'' \rangle.$$

Using the definition of the length and $\|\gamma'\| = 1$, we get

$$\begin{aligned} \left. \frac{dL(\gamma_s)}{ds} \right|_{s=0} &= \int_a^b \left. \frac{\partial}{\partial s} \right|_{s=0} \sqrt{\langle \gamma'_s, \gamma'_s \rangle} \\ &= \frac{1}{2} \int_a^b \left. \frac{\partial}{\partial s} \right|_{s=0} \frac{\langle \gamma'_s, \gamma'_s \rangle}{\sqrt{\langle \gamma', \gamma' \rangle}} \\ &= \int_a^b \left\langle \left. \frac{\partial}{\partial s} \right|_{s=0} \gamma'_s, \gamma' \right\rangle. \end{aligned}$$

To simplify the notation further, define

$$\begin{aligned} \frac{\partial}{\partial t} \gamma_s &:= d\gamma_s \left(\frac{\partial}{\partial t} \right), & \frac{\partial}{\partial s} \gamma_s &:= d\gamma_s \left(\frac{\partial}{\partial s} \right), \\ \frac{\partial}{\partial s} \frac{\partial}{\partial t} \gamma_s &:= \nabla_{\frac{\partial \gamma_s}{\partial s}} \frac{\partial \gamma_s}{\partial t}, & \frac{\partial}{\partial t} \frac{\partial}{\partial s} \gamma_s &:= \nabla_{\frac{\partial \gamma_s}{\partial t}} \frac{\partial \gamma_s}{\partial s}. \end{aligned}$$

Since ∇ is torsion-free and since $[\partial/\partial s, \partial/\partial t] = 0$, we can switch the order of the derivations:

$$\left. \frac{\partial}{\partial s} \right|_{s=0} \gamma'_s = \left. \frac{\partial}{\partial s} \right|_{s=0} \frac{\partial}{\partial t} \gamma_s = \left. \frac{\partial}{\partial t} \frac{\partial}{\partial s} \right|_{s=0} \gamma_s = \frac{\partial}{\partial t} v = \nabla_{\gamma'} v = v'.$$

Thus:

$$\begin{aligned} \left. \frac{dL(\gamma_s)}{ds} \right|_{s=0} &= \int_a^b \left\langle \left. \frac{\partial}{\partial s} \right|_{s=0} \gamma'_s, \gamma' \right\rangle \\ &= \int_a^b \langle v', \gamma' \rangle \\ &= \int_a^b (\langle v, \gamma' \rangle' - \langle v, \gamma'' \rangle) \\ &= \langle v, \gamma' \rangle \Big|_a^b - \int_a^b \langle v, \gamma'' \rangle. \end{aligned}$$

(Note that this proof is a bit sloppy again with ∇ and the kind of vector fields it can operate on.) \square

This result holds for general variations of a curve. We want to show that geodesics are curves of extremal length between two fixed points. So we need to fix the endpoints of the variation. A **variation with fixed endpoints** $\alpha : (-\varepsilon, \varepsilon) \times [a, b] \rightarrow M$ of γ is a variation of γ with $\alpha(s, a) = \gamma(a)$ and $\alpha(s, b) = \gamma(b)$ for all $s \in (-\varepsilon, \varepsilon)$. The variation vector field v of such a variation with fixed endpoints satisfies $v(a) = v(b) = 0$. Now we can finally show the desired result.

Theorem 4: Let (M, g) be a semi-Riemannian manifold, and $\gamma : [a, b] \rightarrow M$ a curve with $\|\gamma'\| = 1$. Then γ is a geodesic if and only if

$$\left. \frac{dL(\gamma_s)}{ds} \right|_{s=0} = 0$$

for all variations with fixed endpoints γ_s of γ .

Proof. \Rightarrow : Let γ be a geodesic. Let γ_s be a variation with fixed endpoints of γ , v its variation vector field. Then we have

$$\frac{dL(\gamma_s)}{ds} \Big|_{s=0} = \underbrace{\langle v, \gamma' \rangle \Big|_a^b}_0 - \int_a^b \underbrace{\langle v, \gamma'' \rangle}_{\parallel 0} = 0.$$

\Leftarrow : Let γ be a curve with $\|\gamma'\| = 1$. We know that γ is a critical point of the length for all variations with fixed endpoints. So it is also a critical point of the length for the variation with fixed endpoints γ_s which comes from the variation vector field $v = f\gamma''$ for $f \in C^\infty(M)$ with $f \geq 0$ and $f(a) = f(b) = 0$.⁵ Then we have

$$0 = \frac{dL(\gamma_s)}{ds} \Big|_{s=0} = \underbrace{\langle v, \gamma' \rangle \Big|_a^b}_0 - \int_a^b \langle v, \gamma'' \rangle = - \int_a^b f \langle \gamma'', \gamma'' \rangle.$$

Since $f \geq 0$ this can only be satisfied if $\gamma'' = 0$. So γ is a geodesic. \square

2.1.8 The Lie Derivative and Killing Fields

In addition to the derivative provided by connections, there is another interesting derivative that is built of the integral curves of vector fields. For a vector field $X \in \Gamma(TM)$ denote by $\phi_t : M \rightarrow M$ the **flow of** X , i.e. the family of maps which take every $p \in M$ a distance t along the unique integral curve of X at p . The **Lie derivative** $\mathcal{L}_X T$ of a tensor field T on M then is

$$\mathcal{L}_X T := \frac{d}{dt} \Big|_{t=0} (\phi_t(T)).$$

So $\mathcal{L}_X T$ is a measure for how much T changes when moved infinitesimally along the integral curves of X . From this definition and the properties of flows, one can find another representation of the Lie derivative of a tensor. Take, for simplicity, a tensor field g of rank 2 (like the metric) and vector fields $\psi, v, w \in \Gamma(TM)$. Then one finds:⁶

$$(\mathcal{L}_\psi g)(v, w) = \psi(g(v, w)) - g(\mathcal{L}_\psi v, w) - g(v, \mathcal{L}_\psi w). \quad (2.7)$$

One key difference between the Lie derivative and the Levi-Civita connection is that the Lie derivative $\mathcal{L}_X T|_p$ depends not only on the value of X at p but also on its value at neighboring points. The Levi-Civita connection depends only on the value at the point, which makes it the preferred derivative in most cases. If we are interested in finding symmetries of the metric tensor, however, the Levi-Civita connection is of no help since the right-hand side of (2.7) vanishes identically when we replace \mathcal{L} with ∇ .

⁵This assumes that for every vector field along a curve there always is a variation with that vector field as its variation vector field. See Gallot, Hulin, and Lafontaine (2004, page 138) for a proof.

⁶See Hawking and Ellis (1973, pages 27ff.) or O'Neill (1983, pages 250ff.) for details. The technique for proving this is identical to that used in section 2.2.4 below.

A vector field $\psi \in \Gamma(TM)$ is called **Killing field** if it leaves the metric invariant under Lie derivation, i.e. if $\mathcal{L}_\psi g = 0$. Due to (2.7), $\mathcal{L}_\psi g = 0$ is equivalent to

$$\psi(g(v, w)) = g(\mathcal{L}_\psi v, w) + g(v, \mathcal{L}_\psi w) \quad \text{for all } v, w \in \Gamma(TM).$$

As a consequence of this and of ∇ being torsion-free there is also a local equivalent for $\mathcal{L}_\psi g = 0$:

$$g_p(\nabla_v \psi, w) + g_p(v, \nabla_w \psi) = 0 \quad \text{for all } v, w \in T_p M \text{ and for all } p \in M.$$

Killing fields ψ denote symmetries of the metric in the sense that their flows ϕ_t leave the metric unchanged:

$$0 = \mathcal{L}_\psi g = \left. \frac{d}{dt} \right|_{t=0} (d\phi_t(g)) = \lim_{t \rightarrow 0} \frac{1}{t} (d\phi_t(g) - g) \quad \Rightarrow \quad d\phi_t(g) = g.$$

2.2 Ricci Calculus

While semi-Riemannian geometry is important for forming an understanding of spacetime physics, it is not very well suited for doing actual computations. This is where the Ricci calculus comes in. This section explains enough of the Ricci calculus to do basic computations with tensors. It first introduces the abstract index notation for multidimensional objects and describes how tensors are represented. It then details the metric tensor and related concepts, including the two important kinds of derivatives. Finally, this section details how geodesics are defined and handled in the context of the Ricci calculus. Most of this is based on von Borzeszkowski and Chrobok (2005/2006), Jänich (2005), and Lovelock and Rund (1975).

2.2.1 The Abstract Index Notation

The abstract index notation is a way to represent multidimensional objects such as vectors or matrices. This representation's main feature is that it deals directly with the components of the concerned objects in some arbitrary but fixed coordinate system. That is, with the abstract index notation, there is always some agreed upon coordinate system and all objects are represented by their components with respect to this coordinate system. The big advantage of this is that we are then dealing with numbers only. Multidimensional objects like matrices can be difficult to deal with in computations: they might not commute for example. Plain numbers, on the other hand, are very easy to handle.

Example 4: A familiar example is the multiplication of vectors and matrices. Suppose we deal with \mathbb{R}^3 . Choose a basis $\{e_1, e_2, e_3\}$ of \mathbb{R}^3 . Then any vector $v \in \mathbb{R}^3$ is completely characterized by its components $v^i \in \mathbb{R}$ with respect to this basis:

$$v^i := v \cdot e_i \quad \Rightarrow \quad v = \sum_{i=1}^3 v^i e_i.$$

Similarly, a 3-by-3 matrix A can be characterized by its components A_i^k . The column vectors A_i of A are given by the images of the basis vectors, and the components of these column vectors determine A completely.

$$A_i := Ae_i \qquad A = \begin{pmatrix} | & | & | \\ A_1 & A_2 & A_3 \\ | & | & | \end{pmatrix}$$

$$A_i^k := A_i \cdot e_k = (Ae_i) \cdot e_k \qquad A_i = \sum_{k=1}^3 A_i^k e_k.$$

The product of the matrix A and the vector v will be a new vector w whose components we can express as a function of the components of A and v :

$$w^i = (Av)^i = \sum_{k=1}^3 A_i^k v_k.$$

Here the advantages of the Ricci calculus start to shine through: while in general $vA \neq Av$, we are free to rearrange the order of A_i^k and v_k on the right side since they are just numbers. The information about whether Av or vA is represented is contained in the position of the summation index.

The product of two matrices A and B is represented in a similar way:

$$(AB)^k_i = \sum_{l=1}^3 A^k_l B^l_i.$$

Again, the order of the terms on the right does not matter. The distinction between AB and BA is conveyed by the position of the summation index.

To simplify the kind of expressions that occurred in the last example, one usually introduces the **summation convention**. It says that indices which appear in pairs of one lower and one upper index are automatically summed over. Latin indices conventionally range from 1 to 3, while Greek indices range from 0 to 3. So for example, we have:

$$A^k_l B^l_i = \sum_{l=1}^3 A^k_l B^l_i,$$

$$F^\mu_\nu v^\nu = \sum_{\nu=0}^3 F^\mu_\nu v^\nu,$$

$$W^\rho_\kappa v^\kappa u_\rho = \sum_{\rho=0}^3 \sum_{\kappa=0}^3 W^\rho_\kappa v^\kappa u_\rho.$$

2.2.2 Tensors and their Transformation

In Ricci calculus, tensors are thought of as multilinear maps that operate on vector fields and their duals. In contrast to the tensor concept of section 2.1.4, there are now different kinds of tensors taking different numbers of vector fields and dual vector fields. Nevertheless, tensors in Ricci calculus are still cross sections of certain fibre bundles called tensor bundles. The following will explain all this in more detail.

As we saw in section 2.1.2, a chart (U, x) about a point p of a manifold M induces a coordinate system in a neighborhood of p and a basis of the tangent space T_pM . In the notation of Ricci calculus, the coordinate functions $\{x^\mu\}$ of x provide us with the canonical basis $\{\partial_\mu^p\}$ of T_pM and we can write every $v \in T_pM$ as

$$v = v^\mu \partial_\mu^p \quad \text{with } v^\mu = v(x^\mu) \in \mathbb{R}.$$

With respect to another chart (\tilde{U}, \tilde{x}) about p , we can use the chain rule to get

$$v = \tilde{v}^\mu \tilde{\partial}_\mu^p = \tilde{v}^\mu \left. \frac{\partial}{\partial \tilde{x}^\mu} \right|_p = \tilde{v}^\mu \left. \frac{\partial x^\nu}{\partial \tilde{x}^\mu} \frac{\partial}{\partial x^\nu} \right|_p = v^\nu \partial_\nu^p,$$

where

$$v^\nu = \tilde{v}^\mu A^\nu{}_\mu(p) := \tilde{v}^\mu \left. \frac{\partial x^\nu}{\partial \tilde{x}^\mu} \right|_p.$$

So under a change of charts $(U, x) \rightarrow (\tilde{U}, \tilde{x})$, the components of a tangent vector transform with the Jacobian $A^\nu{}_\mu(p) = \partial x^\nu / \partial \tilde{x}^\mu|_p$ of the coordinate functions. In Ricci calculus, quantities that satisfy this transformation law are called **contravariant tensors**. In fact, contravariance is often used to *define* tangent vectors and thus tangent space. This is an equivalent approach to the one described in earlier sections.

Vector fields $\psi \in \Gamma(TM)$ can be treated in a similar way to get $\psi = \psi^\mu \partial_\mu$ where $\psi^\mu = \psi(x^\mu) \in C^\infty(M)$ and where $\{\partial_\mu\}$ are the canonical basis fields induced by a chart. Under a change of charts $(U, x) \rightarrow (\tilde{U}, \tilde{x})$, the components ψ^μ are found to transform with the Jacobian $A^\nu{}_\mu = \partial x^\nu / \partial \tilde{x}^\mu$ too.

The same general approach can also be applied to the dual space T_p^*M of T_pM . This is the space of all linear maps $\omega : T_pM \rightarrow \mathbb{R}$. In section 2.1.2 we already encountered one such map: $d_p f$ for $f \in C^\infty(M)$. It maps $v \in T_pM$ to $d_p f(v) = v(f) \in \mathbb{R}$. Now choose a chart (U, x) about p and set $f = x^\mu$ and $v = \partial_\nu^p$. Then we see that

$$d_p x^\mu(\partial_\nu^p) = \partial_\nu^p(x^\mu) = \left. \frac{\partial x^\mu}{\partial x^\nu} \right|_{x(p)} = \delta_\nu^\mu.$$

So $\{d_p x^\mu\}$ is dual to $\{\partial_\mu^p\}$ and therefore $\{d_p x^\mu\}$ is a basis of T_p^*M . Any $\omega \in T_p^*M$ can now be written as $\omega = \omega_\mu d_p x^\mu$ with $\omega_\mu = \omega(\partial_\mu^p) \in \mathbb{R}$. A similar computation to the one done above shows that, under a change of charts $(U, x) \rightarrow (\tilde{U}, \tilde{x})$, the components ω_μ transform in the following way:

$$\omega_\mu = \tilde{\omega}_\nu \tilde{A}^\nu{}_\mu(p) := \tilde{\omega}_\nu \left. \frac{\partial \tilde{x}^\nu}{\partial x^\mu} \right|_p.$$

That is, under a change of charts, the components of elements of the dual space T_p^*M transform with the *inverse* Jacobian $\bar{A}^\nu_\mu(p)$ of the coordinate functions. In Ricci calculus, quantities that satisfy this transformation law are called **covariant tensors**.

A very important relation emerges when we apply a covariant tensor $\omega \in T_p^*M$ to a contravariant tensor $v \in T_pM$:

$$\omega(v) = \omega_\mu dx^\mu(v^\nu \partial_\nu) = \omega_\mu v^\nu dx^\mu(\partial_\nu) = \omega_\mu v^\nu \delta^\mu_\nu = \omega_\mu v^\mu$$

So to get $\omega(v)$ we just need to sum the products of their components. How does the value of $\omega(v) = \omega_\mu v^\mu$ change under a change of charts $(U, x) \rightarrow (\tilde{U}, \tilde{x})$?

$$\omega_\mu v^\mu = (\tilde{\omega}_\nu \bar{A}^\nu_\mu(p)) \left(\tilde{v}^\lambda A^\mu_\lambda(p) \right) = \tilde{\omega}_\nu \tilde{v}^\lambda \bar{A}^\nu_\mu(p) A^\mu_\lambda(p) = \tilde{\omega}_\nu \tilde{v}^\lambda \delta^\nu_\lambda = \tilde{\omega}_\nu \tilde{v}^\nu.$$

So, since μ on the left side and ν on the right side are just summation indices and therefore interchangeable, $\omega(v) = \omega_\mu v^\mu$ does not depend on the chosen chart. Quantities like this that are invariant under coordinate transformations are called **scalars** or **invariants** in Ricci calculus.

With T_p^*M defined as the dual of T_pM , it is natural to wonder what the dual $T_p^{**}M$ of T_p^*M is. Any $\tau \in T_p^{**}M$ maps a covariant tensor $\omega \in T_p^*M$ to a number. As we have seen above, a covariant tensor ω maps a contravariant tensor $v \in T_pM$ to a number. This viewpoint can also be reversed, however. We can simply define $v(\omega) := \omega(v)$. Thus $v \in T_p^{**}M$ and $T_pM \subset T_p^{**}M$. In fact, it can be shown that T_pM and $T_p^{**}M$ are isomorphic, i.e. $T_pM \cong T_p^{**}M$, provided that the dimension of M is finite. So a contravariant tensor can be thought of as operating on a covariant tensor.

We will often need quantities that operate on more than one tensor, possibly on different kinds of tensors. These kinds of objects can be described with the tensor product. Given a map $f : T_pM \times \cdots \times T_pM \rightarrow \mathbb{R}$ that is linear in every of its s arguments, and a map $g : T_p^*M \times \cdots \times T_p^*M \rightarrow \mathbb{R}$ that is also linear in every of its r arguments, the **tensor product** $f \otimes g$ is defined by

$$f \otimes g : \overbrace{T_pM \times \cdots \times T_pM}^s \times \overbrace{T_p^*M \times \cdots \times T_p^*M}^r \rightarrow \mathbb{R}$$

$$(f \otimes g)(v_1, \dots, v_s, \omega_1, \dots, \omega_r) = f(v_1, \dots, v_s) g(\omega_1, \dots, \omega_r).$$

So $f \otimes g$ operates on $s + r$ tensors by passing the first s contravariant tensors to f and the other r covariant tensors to g .

The space $\mathcal{T}_s^r(M, p)$ of all those multilinear functions is called **tensor space at p** and is given by

$$\mathcal{T}_s^r(M, p) = \overbrace{T_p^*M \otimes \cdots \otimes T_p^*M}^s \otimes \overbrace{T_pM \otimes \cdots \otimes T_pM}^r$$

$$= C^\infty(\underbrace{T_pM \times \cdots \times T_pM}_s \times \underbrace{T_p^*M \times \cdots \times T_p^*M}_r).$$

So $\mathcal{T}_1^0(M, p) = C^\infty(T_p M) = T_p^* M$ is the space of all covariant tensors, and $\mathcal{T}_0^1(M, p) = C^\infty(T_p^* M) = T_p M$ is the space of all contravariant tensors. If $\{\partial_\mu^p\}$ and $\{d_p x^\nu\}$ denote the bases of $T_p M$ and $T_p^* M$ induced by the chart (U, x) about p , then

$$\{d_p x^{\nu_1} \otimes \cdots \otimes d_p x^{\nu_s} \otimes \partial_{\mu_1}^p \otimes \cdots \otimes \partial_{\mu_r}^p\}$$

forms a basis of $\mathcal{T}_s^r(M, p)$. That is, every $T \in \mathcal{T}_s^r(M, p)$ can be written as

$$T = T^{\mu_1 \cdots \mu_r}_{\nu_1 \cdots \nu_s} d_p x^{\nu_1} \otimes \cdots \otimes d_p x^{\nu_s} \otimes \partial_{\mu_1}^p \otimes \cdots \otimes \partial_{\mu_r}^p,$$

where $T^{\mu_1 \cdots \mu_r}_{\nu_1 \cdots \nu_s} \in \mathbb{R}$ are called **components** of T with respect to the chart (U, x) . They are given by

$$T^{\mu_1 \cdots \mu_r}_{\nu_1 \cdots \nu_s} = T(\partial_{\nu_1}^p, \dots, \partial_{\nu_s}^p, d_p x^{\mu_1}, \dots, d_p x^{\mu_r}).$$

With this in mind, it is easy to see that the elements of $\mathcal{T}_s^r(M, p)$ satisfy the following transformation law:

$$T^{\mu_1 \cdots \mu_r}_{\nu_1 \cdots \nu_s} = \tilde{T}^{\rho_1 \cdots \rho_r}_{\sigma_1 \cdots \sigma_s} A^{\mu_1}_{\rho_1} \cdots A^{\mu_r}_{\rho_r} \bar{A}^{\sigma_1}_{\nu_1} \cdots \bar{A}^{\sigma_s}_{\nu_s} \Big|_p$$

Consequently, Ricci calculus calls elements of $\mathcal{T}_s^r(M, p)$ **tensors of type** (r, s) , where r denotes the contravariant and s the covariant rank.

When we collect the $\mathcal{T}_s^r(M, p)$ for all $p \in M$, we get the **tensor bundle** $\mathcal{T}_s^r(M)$:

$$\mathcal{T}_s^r(M) := \bigcup_{p \in M} \mathcal{T}_s^r(M, p).$$

The cross sections $\Gamma(\mathcal{T}_s^r(M))$ of $\mathcal{T}_s^r(M)$ are called **tensor fields**. They assign to every $p \in M$ a tensor of type (r, s) at p . And thus we have finally reached the point where we can marry the tensor concept of semi-Riemannian geometry and that of Ricci calculus. Recall that in section 2.1.4, tensors were defined as cross sections ω which assign to every $p \in M$ a multilinear k -form $\omega_p : T_p M \times \cdots \times T_p M \rightarrow E_p$ where E is a vector bundle over M . Choose $E = TM$ and we see that

$$\omega_p \in T_p^* M \otimes \cdots \otimes T_p^* M \otimes T_p M = \mathcal{T}_k^1(M, p).$$

Thus $\omega \in \Gamma(\mathcal{T}_k^1(M))$. So the tensors of semi-Riemannian geometry are the tensor fields of rank $(1, k)$ of Ricci calculus.

Since there is such a close connection between a tensor $T \in \mathcal{T}_s^r(M, p)$ and its components $T^{\mu_1 \cdots \mu_r}_{\nu_1 \cdots \nu_s}$, it is conventional to use both symbols interchangeably. Thus, the collection of components $T^{\mu_1 \cdots \mu_r}_{\nu_1 \cdots \nu_s}$ is identified with T . Similarly, a tensor field $S \in \Gamma(\mathcal{T}_s^r(M))$ is identified with its components $S^{\mu_1 \cdots \mu_r}_{\nu_1 \cdots \nu_s}$.

2.2.3 The Metric

In section 2.1.5, we defined a metric g to be a tensor which assigns to every $p \in M$ an inner product $g_p : T_p M \times T_p M \rightarrow \mathbb{R}$. Thus, in Ricci calculus, $g \in \Gamma(\mathcal{T}_2^0(M))$ is represented by the components $g_{\mu\nu}$:

$$g = g_{\mu\nu} dx^\mu \otimes dx^\nu \quad \text{for some chart } (U, x).$$

So the metric $g_{\mu\nu}$ assigns to every $p \in M$ a tensor $g_{\mu\nu}(p) \in \mathcal{T}_2^0(M, p)$ of type $(0, 2)$ which in turn maps two covariant tensors $v^\mu(p), w^\nu(p) \in \mathcal{T}_1^0(M, p)$ to a number. Or, more conventionally, we can think of $g_{\mu\nu}$ as operating on tensor fields $v^\mu, w^\nu \in \Gamma(\mathcal{T}_1^0(M))$ and yielding a function $g_{\mu\nu}v^\mu w^\nu \in C^\infty(M)$. This point of view makes it easy to see how exactly $g_{\mu\nu}$ relates to g :

$$\begin{aligned} g(v, w) &= (g_{\mu\nu} dx^\mu \otimes dx^\nu)(v, w) \\ &= g_{\mu\nu} dx^\mu (v^\rho \partial_\rho) dx^\nu (w^\sigma \partial_\sigma) \\ &= g_{\mu\nu} v^\rho w^\sigma \delta_\rho^\mu \delta_\sigma^\nu \\ &= g_{\mu\nu} v^\mu w^\nu. \end{aligned}$$

The symmetry of g in its arguments translates to the symmetry of $g_{\mu\nu}$ in its indices:

$$g(v, w) = g(w, v) \iff g_{\mu\nu} = g_{\nu\mu}.$$

Since $g_{\mu\nu}$ has rank $(0, 2)$, its application to two tensors v^μ, w^ν of rank $(1, 0)$ yields a quantity $g_{\mu\nu}v^\mu w^\nu$ which is invariant under coordinate transformations. We have encountered another invariant quantity before: $\omega_\mu v^\mu$ where ω_μ is a tensor of rank $(0, 1)$. It turns out that there is a connection between these two kinds of expressions. Consider $g_{\mu\nu}v^\mu$, i.e. leave one argument of $g_{\mu\nu}$ empty. Since it takes another contravariant tensor, we have $g_{\mu\nu}v^\mu \in \Gamma(\mathcal{T}_1^0(M))$. So $g_{\mu\nu}v^\mu$ gives us a tensor field of rank $(0, 1)$. In fact, the following is true: there always is exactly one $v^\mu \in \Gamma(\mathcal{T}_1^0(M))$ for every $\omega_\nu \in \Gamma(\mathcal{T}_1^0(M))$ with $\omega_\nu = g_{\mu\nu}v^\mu$. So the metric $g_{\mu\nu}$ induces an isomorphism

$$\begin{aligned} \Gamma(\mathcal{T}_1^0(M)) = \Gamma(TM) &\longleftrightarrow \Gamma(T^*M) = \Gamma(\mathcal{T}_1^0(M)) \\ v^\mu &\longleftrightarrow g_{\mu\nu}v^\mu. \end{aligned} \tag{2.8}$$

This is known as the Riesz representation theorem.

Due to the close relation between a covariant tensor ω_μ and its representing contravariant tensor v_ν , Ricci calculus uses the same symbol for both entities: $v_\nu = g_{\mu\nu}v^\mu$. So, graphically speaking, the metric can be used to “**pull down indices**” of contravariant tensors and turn them into covariant tensors.

What about the inverse of this operation? It would assign to a covariant tensor $\omega_\mu = g_{\mu\nu}v^\nu$ its representing contravariant tensor v^ν . It turns out that this is achieved by the tensor $g^{\mu\nu}$ defined as the matrix inverse of $g_{\mu\nu}$:

$$g^{\mu\nu}g_{\nu\lambda} = \delta_\lambda^\mu. \tag{2.9}$$

Because then we have

$$g^{\mu\nu}\omega_\mu = g^{\mu\nu}g_{\mu\sigma}v^\sigma = v^\nu.$$

The tensor $g^{\mu\nu}$ is often called the **dual** or **inverse metric**. This is not to be confused with the inverse of the metric: the metric $g_{\mu\nu}$ is not injective, so it does not even have an inverse. Instead, $g^{\mu\nu}$ can be thought of as the map that gives rise to the \leftarrow part of the isomorphism (2.8).

Due to the close connection between ω_μ and its representing contravariant tensor v^ν , both are assigned the same symbol: $g^{\mu\nu}\omega_\mu = \omega^\nu$. Hence we see that $g^{\mu\nu}$ can be used to “*pull up indices*”. From the definition (2.9) we also have $g^{\mu\nu} = g^{\mu\rho}g^{\nu\sigma}g_{\rho\sigma}$. So the previous definitions are indeed consistent and $g^{\mu\nu}$ is obtained by pulling up the indices of $g_{\mu\nu}$.

2.2.4 The Derivatives

We already know one kind of derivative: the partial derivatives ∂_μ that are induced by a chart (U, x) and that form a basis for contravariant tensors. We can apply ∂_μ to v^ν to obtain a new quantity $\partial_\mu v^\nu$ with two indices. For brevity, a new syntax is often used for these kinds of expressions:

$$v^\nu{}_{,\mu} := \partial_\mu v^\nu.$$

How does this quantity transform under a change of coordinates?

$$\begin{aligned} v^\nu{}_{,\mu} &= \frac{\partial}{\partial x^\mu} v^\nu \\ &= \frac{\partial \tilde{x}^\sigma}{\partial x^\mu} \frac{\partial}{\partial \tilde{x}^\sigma} \left(\frac{\partial x^\nu}{\partial \tilde{x}^\rho} \tilde{v}^\rho \right) \\ &= \frac{\partial \tilde{x}^\sigma}{\partial x^\mu} \left(\frac{\partial^2 x^\nu}{\partial \tilde{x}^\sigma \partial \tilde{x}^\rho} \tilde{v}^\rho + \frac{\partial x^\nu}{\partial \tilde{x}^\rho} \frac{\partial}{\partial \tilde{x}^\sigma} \tilde{v}^\rho \right) \\ &= \frac{\partial \tilde{x}^\sigma}{\partial x^\mu} \frac{\partial^2 x^\nu}{\partial \tilde{x}^\sigma \partial \tilde{x}^\rho} \tilde{v}^\rho + \frac{\partial \tilde{x}^\sigma}{\partial x^\mu} \frac{\partial x^\nu}{\partial \tilde{x}^\rho} \tilde{v}^\rho{}_{,\sigma}. \end{aligned} \tag{2.10}$$

This shows that $v^\nu{}_{,\mu}$ are *not* the components of a tensor, due to the first term on the last line. In order to define a derivative that yields a tensor, we need to amend the bare $v^\nu{}_{,\mu}$ in such a way that this first term does not occur when changing coordinates.

It turns out that this can be achieved with the concept of connections introduced in section 2.1.6. There, a connection was defined as a linear map $\nabla : \Gamma(TM) \times \Gamma(E) \rightarrow \Gamma(E)$ for some vector bundle E . Choose $E = TM$. Then we can think of ∇ as a map $\nabla : \Gamma(TM) \times \Gamma(TM) \times \Gamma(T^*M) \rightarrow \mathbb{R}$. Note that $\nabla \notin \mathcal{T}_1^2(M)$ since ∇ is not $C^\infty(M)$ -linear in its second argument. When we fix the second argument, however, we do get a tensor:

$$v \in \Gamma(TM) = \mathcal{T}_0^1(M) \Rightarrow \nabla v \in \mathcal{T}_1^1(M).$$

This new tensor ∇v is called the **covariant derivative of v** . When we fill in the first argument of ∇v with $w \in \mathcal{T}_0^1(M)$ we get $\nabla_w v$, the **covariant derivative of v in the direction w** . And filling in the last argument with $\omega \in \mathcal{T}_1^0(M)$, we get $(\nabla_w v)(\omega) = \omega(\nabla_w v)$.

On a chart (U, x) , the connection is determined by its components $\Gamma_{\nu\lambda}^\mu$ on the basis $\{\partial_\mu\}$ and its dual $\{dx^\mu\}$:

$$\Gamma_{\nu\lambda}^\mu := (\nabla_{\partial_\nu} \partial_\lambda)(dx^\mu) \Leftrightarrow \nabla \partial_\lambda = \Gamma_{\nu\lambda}^\mu dx^\nu \otimes \partial_\mu.$$

The components $\Gamma_{\nu\lambda}^\mu$ are called **Christoffel symbols of ∇** . The relation $\nabla_u(fv) = u(f)v + f\nabla_u v$ from the definition of a connection can be expressed as

$$\nabla(fv) = df \otimes v + f\nabla v$$

for all $f \in C^\infty(M)$, $v \in \mathcal{T}_0^1(M)$. Thus, for any $v \in \mathcal{T}_0^1(M)$, we have

$$\nabla v = \nabla(v^\mu \partial_\mu) = dv^\mu \otimes \partial_\mu + v^\mu \Gamma_{\nu\mu}^\lambda dx^\nu \otimes \partial_\lambda.$$

So we see that the components $v^\mu_{;\nu}$ of $\nabla v = v^\mu_{;\nu} dx^\nu \otimes \partial_\mu$ are given by

$$v^\mu_{;\nu} = \frac{\partial v^\mu}{\partial x^\nu} + \Gamma_{\nu\lambda}^\mu v^\lambda = v^\mu_{,\nu} + \Gamma_{\nu\lambda}^\mu v^\lambda.$$

In Ricci calculus, $v^\mu_{;\nu}$ is called the **covariant derivative of the contravariant tensor v^μ** . The covariant derivative $\nabla_w v$ of v in the direction w is given by $w^\nu v^\mu_{;\nu}$ in this notation.

Under a change of coordinates with Jacobian $A^\nu_\mu := \partial x^\nu / \partial \tilde{x}^\mu$ and inverse Jacobian $\bar{A}^\nu_\mu := \partial \tilde{x}^\nu / \partial x^\mu$, we can use the properties of the connection to obtain

$$\begin{aligned} \tilde{\Gamma}_{\nu\lambda}^\mu &= (\nabla_{\tilde{\partial}_\nu} \tilde{\partial}_\lambda)(d\tilde{x}^\mu) \\ &= (\nabla_{A^\rho_\nu \partial_\rho} A^\sigma_\lambda \partial_\sigma)(\bar{A}^\mu_\kappa dx^\kappa) \\ &= \bar{A}^\mu_\kappa A^\rho_\nu \left[(\partial_\rho A^\sigma_\lambda) \partial_\sigma + A^\sigma_\lambda \nabla_{\partial_\rho} \partial_\sigma \right] (dx^\kappa) \\ &= \bar{A}^\mu_\kappa A^\rho_\nu \left[\partial_\rho A^\kappa_\lambda + A^\sigma_\lambda \Gamma_{\rho\sigma}^\kappa \right] \\ &= \bar{A}^\mu_\kappa \left[\tilde{\partial}_\rho A^\kappa_\lambda + A^\rho_\nu A^\sigma_\lambda \Gamma_{\rho\sigma}^\kappa \right] \\ &= \frac{\partial \tilde{x}^\mu}{\partial x^\kappa} \left[\frac{\partial^2 x^\kappa}{\partial \tilde{x}^\rho \partial \tilde{x}^\lambda} + \frac{\partial x^\rho}{\partial \tilde{x}^\nu} \frac{\partial x^\sigma}{\partial \tilde{x}^\lambda} \Gamma_{\rho\sigma}^\kappa \right]. \end{aligned} \tag{2.11}$$

Comparing this with equation (2.10), we see that $v^\mu_{;\nu}$ does indeed transform like a tensor of rank (1, 1):

$$v^\mu_{;\nu} = \frac{\partial x^\mu}{\partial \tilde{x}^\kappa} \frac{\partial \tilde{x}^\rho}{\partial x^\nu} \tilde{v}^\kappa_{;\rho}.$$

We can define the covariant derivative of tensors of arbitrary rank by demanding the following rules:

1. If $T \in \mathcal{T}_s^r(M)$, then $\nabla T \in \mathcal{T}_{s+1}^r(M)$.
2. ∇ commutes with contraction. This means that any tensor equation involving ∇ still holds when we contract $\omega \otimes v \rightarrow \omega(v)$ for any $\omega \in \mathcal{T}_1^0(M)$, $v \in \mathcal{T}_0^1(M)$.
3. The Leibniz rule holds for arbitrary tensors T, S :

$$\nabla(S \otimes T) = (\nabla S) \otimes T + S \otimes (\nabla T).$$

4. For any function $f \in C^\infty(M)$, we have $\nabla f = df$.

We can use these rules to find the covariant derivative of a covariant tensor ω . First, use the Leibniz rule for $\omega \otimes \partial_\mu$:

$$\nabla(\omega \otimes \partial_\mu) = (\nabla\omega) \otimes \partial_\mu + \omega \otimes (\nabla\partial_\mu).$$

Then apply the contraction $\omega \otimes v \rightarrow \omega(v)$:

$$\nabla(\omega(\partial_\mu)) = (\nabla\omega)(\partial_\mu) + \omega(\nabla\partial_\mu).$$

Solve for $(\nabla\omega)(\partial_\mu)$ and insert ∂_ν for the free argument:

$$\begin{aligned} (\nabla_{\partial_\nu}\omega)(\partial_\mu) &= \nabla_{\partial_\nu}(\omega(\partial_\mu)) - \omega(\nabla_{\partial_\nu}\partial_\mu) \\ &= \partial_\nu(\omega(\partial_\mu)) - \omega(\Gamma_{\nu\mu}^\lambda\partial_\lambda) \\ &= \partial_\nu(\omega(\partial_\mu)) - \Gamma_{\nu\mu}^\lambda\omega(\partial_\lambda). \end{aligned}$$

Thus, the *covariant derivative* $\omega_{\mu;\nu}$ *of a covariant tensor* ω_μ is given by

$$\omega_{\mu;\nu} = \omega_{\mu,\nu} - \Gamma_{\nu\mu}^\lambda\omega_\lambda.$$

It should be clear from the derivation of this expression that $\omega_{\mu;\nu}$ is indeed a tensor, but it can also be checked manually by using the transformation properties (2.11) of the Christoffel symbols.

The same procedure can be used to find the covariant derivative of an arbitrary tensor $T \in \mathcal{T}_s^r(M)$. We arrive at

$$\begin{aligned} T^{\alpha\dots\beta}_{\mu\dots\nu;\lambda} &= T^{\alpha\dots\beta}_{\mu\dots\nu,\lambda} \\ &\quad + \Gamma_{\lambda\rho}^\alpha T^{\rho\dots\beta}_{\mu\dots\nu} + \dots + \Gamma_{\lambda\sigma}^\beta T^{\alpha\dots\sigma}_{\mu\dots\nu} \\ &\quad - \Gamma_{\lambda\mu}^\kappa T^{\alpha\dots\beta}_{\kappa\dots\nu} - \dots - \Gamma_{\lambda\nu}^\xi T^{\alpha\dots\beta}_{\mu\dots\xi}. \end{aligned}$$

Up to now we have dealt with general connections on a manifold independent of any metric that might also be present. But remember from section 2.1.6 that for every metric g there is exactly one torsion-free connection that is metric preserving: the Levi-Civita connection ∇ of g . A connection is metric preserving if

$$u(g(v, w)) = g(\nabla_u v, w) + g(v, \nabla_u w)$$

for every $u, v, w \in \mathcal{T}_0^1(M)$. With what we have shown above, this is equivalent to:

$$\nabla g = 0 \quad \text{and} \quad g_{\alpha\beta;\gamma} = 0.$$

That is, a connection is metric preserving if the corresponding covariant derivative of the metric vanishes. When a metric is present, the tensor contraction mentioned above is given by the isomorphism (2.8). So the rules 2 and 3 which we demanded from a connection above are satisfied by the Levi-Civita connection in a natural way.

In section 2.1.6 we also showed that the Levi-Civita connection is determined by the Koszul formula (2.6):

$$2g(\nabla_u v, w) = u(g(v, w)) + v(g(w, u)) - w(g(u, v)) \\ + g([u, v], w) - g([u, w], v) - g([v, w], u).$$

Upon choosing basis tensors for u, v, w we can use this to obtain the Christoffel symbols for ∇ :

$$2g(\nabla_{\partial_\mu} \partial_\nu, \partial_\lambda) = \partial_\mu(g(\partial_\nu, \partial_\lambda)) + \partial_\nu(g(\partial_\lambda, \partial_\mu)) - \partial_\lambda(g(\partial_\mu, \partial_\nu)) \\ + g(\underbrace{[\partial_\mu, \partial_\nu]}_0, \partial_\lambda) - g(\underbrace{[\partial_\mu, \partial_\lambda]}_0, \partial_\nu) - g(\underbrace{[\partial_\nu, \partial_\lambda]}_0, \partial_\mu) \\ = \partial_\mu(g(\partial_\nu, \partial_\lambda)) + \partial_\nu(g(\partial_\lambda, \partial_\mu)) - \partial_\lambda(g(\partial_\mu, \partial_\nu)).$$

Or, in coordinates:

$$2g_{\rho\lambda}\Gamma_{\mu\nu}^\rho = g_{\nu\lambda,\mu} + g_{\lambda\mu,\nu} - g_{\mu\nu,\lambda} \Leftrightarrow \Gamma_{\mu\nu}^\tau = \frac{1}{2}g^{\tau\lambda}(g_{\nu\lambda,\mu} + g_{\lambda\mu,\nu} - g_{\mu\nu,\lambda}).$$

Given the metric $g_{\mu\nu}$ we can now calculate any covariant derivative of any tensor.

In section 2.1.6, we defined the curvature tensor R of a connection as

$$R(v, w)u = \nabla_v(\nabla_w u) - \nabla_w(\nabla_v u) - \nabla_{[v, w]}u$$

for $v, w \in \Gamma(TM)$ and $u \in \Gamma(E)$. With $E = TM$, this yields a tensor $R \in \mathcal{T}_1^3(M)$. If ∇ is the Levi-Civita connection, it is torsion-free: $[v, w] = \nabla_v w - \nabla_w v$. Thus, in coordinates, we can write R as

$$R^\alpha{}_{\beta\gamma\delta}v^\beta w^\gamma u^\delta = (u^\alpha{}_{;\mu}w^\mu)_{;\nu}v^\nu - (u^\alpha{}_{;\lambda}v^\lambda)_{;\rho}w^\rho - (w^\sigma{}_{;\xi}v^\xi - v^\sigma{}_{;\chi}w^\chi)u^\alpha{}_{;\sigma} \\ = (u^\alpha{}_{;\mu;\nu} - u^\alpha{}_{;\nu;\mu})v^\nu w^\mu.$$

And since v, w are arbitrary:

$$R^\alpha{}_{\beta\gamma\delta}u^\delta = u^\alpha{}_{;\gamma;\beta} - u^\alpha{}_{;\beta;\gamma}.$$

2.2.5 Geodesics and Killing Fields

In section 2.1.7 we defined geodesics as those curves $\gamma \in C^\infty(M)$ which satisfy $\nabla_{\gamma'}\gamma' = 0$, i.e. curves whose tangent vector is parallel-transported. As always in Ricci calculus, we choose some chart (U, x) of M and then consider the components $\{\gamma^\mu = x^\mu \circ \gamma\}$ of γ with respect to that chart. With $v^\mu = \gamma^{\mu'}$, the condition for γ to be a geodesic reads

$$0 = v^\mu{}_{;\nu}v^\nu \\ = v^\mu{}_{,\nu}v^\nu + \Gamma_{\nu\lambda}^\mu v^\lambda v^\nu \\ = \left(\frac{d}{dx_\nu} \frac{d\gamma^\mu(\tau)}{d\tau} \right) \frac{d\gamma^\nu(\tau)}{d\tau} + \Gamma_{\nu\lambda}^\mu \frac{d\gamma^\lambda(\tau)}{d\tau} \frac{d\gamma^\nu(\tau)}{d\tau} \\ = \frac{d^2\gamma^\mu(\tau)}{d\tau^2} + \Gamma_{\nu\lambda}^\mu \frac{d\gamma^\lambda(\tau)}{d\tau} \frac{d\gamma^\nu(\tau)}{d\tau}. \tag{2.12}$$

This is the *geodesic equation* in Ricci calculus, consisting of n ordinary differential equations for the n components of γ .

One of the defining equations of Killing fields, as was shown in section 2.1.8, is

$$g_p(\nabla_v \psi, w) + g_p(v, \nabla_w \psi) = 0 \quad \text{for all } v, w \in T_p M \text{ and for all } p \in M.$$

In coordinates, this is known as the *Killing equation* and takes the remarkably simple form

$$\psi_{\mu;\nu} + \psi_{\nu;\mu} = 0.$$

3 General Relativity

The theory of General Relativity asserts that our universe can be thought of as a four dimensional entity called spacetime. This spacetime is a Lorentzian manifold, a special case of a semi-Riemannian manifold as described in section 2.1.5. So in this chapter, we use the formalisms developed in the previous chapter to describe the structure of the universe. We also look at the field equations of General Relativity which specify how the matter distribution in the universe determines its metric. This chapter is mostly based on von Borzeszkowski and Chrobok (2005/2006), Hawking and Ellis (1973), and occasionally on Beem, Ehrlich, and Easley (1996).

3.1 Spacetime as a Lorentzian Manifold

In General Relativity the strict distinction between space and time as we know it from everyday life is abandoned in favor of the four dimensional spacetime which subsumes space and time. The spacetime is described by a *Lorentzian manifold*, i.e. a tuple (M, g) of a differentiable manifold M together with an indefinite, non-degenerate metric g which gives rise to the Levi-Civita connection and its curvature tensor. The key insight in General Relativity is that the curvature of a spacetime is what creates gravitation. Gravitational forces result from curvature. And the field equations, which we will come to soon, tell us that matter determines the metric and thus the curvature. So matter in a spacetime creates curvature, and curvature in turn determines how matter moves on a large scale.

Another fundamental axiom of General Relativity is the *equivalence principle*. Greatly simplified, it says that all frames of reference should be equivalent, i.e. that every physical law needs to be covariant under arbitrary coordinate transformations. When we formulate the physical laws as tensor equations on a Lorentzian manifold, this requirement is automatically fulfilled.

A popular way to specify the metric g of a spacetime M is to give its components in a particular chart (U, x) . This is often done by specifying the *line element* $ds^2 = g_{\mu\nu}dx^\mu dx^\nu$, where the tensor product sign \otimes is omitted for convenience. Reinstating \otimes , we see that $ds^2 = g_{\mu\nu}dx^\mu \otimes dx^\nu$ and thus $ds^2 = g$. So ds^2 is just another name for g . As an example of this syntax, consider the *Minkowski spacetime* in the coordinates (t, x, y, z) :

$$\begin{aligned} ds^2 &= dt^2 - dx^2 - dy^2 - dz^2 \\ g_{\mu\nu} &= \text{diag}(1, -1, -1, -1). \end{aligned} \tag{3.1}$$

Another example, the *Schwarzschild spacetime* in the coordinates (t, r, θ, ϕ) :

$$\begin{aligned} ds^2 &= \left(1 - \frac{r_s}{r}\right) dt^2 - \left(1 - \frac{r_s}{r}\right)^{-1} dr^2 - r^2 (d\theta^2 + \sin^2 \theta d\phi^2) \\ g_{\mu\nu} &= \text{diag} \left(\left(1 - \frac{r_s}{r}\right), -\left(1 - \frac{r_s}{r}\right)^{-1}, -r^2, -r^2 \sin^2 \theta \right), \end{aligned} \quad (3.2)$$

where $t, r \in \mathbb{R}$, $\theta \in [0, \pi]$, and $\phi \in [0, 2\pi]$ and where $\theta = 0$ and $\theta = \pi$ are identified just like $\phi = 0$ and $\phi = 2\pi$. For fixed t and r , the metric describes ordinary spheres. The metric degenerates when $\theta = 0$ or $\theta = \pi$ (since $\sin^2 \theta = 0$ there), so these slices would have to be cut out if we want to have a proper manifold. There are similar problems with $r = 0$ or $r = r_s$.

These so called ‘‘singularities’’ are points in the spacetime where a particular coordinate representation of a metric is singular. This means that at those points, the metric becomes degenerate or ill-defined due to some component vanishing or diverging. For example, the Schwarzschild spacetime (3.2) is singular at $r = 0$ and $r = r_s$. These singularities can be of two basic types: they can be coordinate singularities or physical singularities.

Coordinate singularities are singularities that are due to an inadequate choice of coordinates. They have no direct physical effect, the spacetime is perfectly regular there. Coordinate singularities can be removed by switching to another set of coordinates. As an example of this type of singularity, consider the Euclidean plane ($M = \mathbb{R}^2, g$) in polar coordinates (r, ϕ) :

$$ds^2 = dr^2 + r^2 d\phi^2.$$

At $r = 0$, this coordinate representation becomes singular. But from the Cartesian representation

$$ds^2 = dx^2 + dy^2$$

with $x = r \cos \phi$ and $y = r \sin \phi$, we know that the plane is perfectly regular at the origin $(r = 0, \phi) = (x = 0, y = 0)$. The $r = r_s$ singularity of the Schwarzschild spacetime is another example of a coordinate singularity.

Note that while coordinate singularities do not have immediate physical consequences, they do sometimes signify interesting features. The Schwarzschild singularity just mentioned is an example: $r = r_s$ denotes the hypersurface beyond which no light can escape from the black hole. Rosen (1985) provides more interesting arguments why coordinate singularities should not be dismissed easily.

Physical singularities are points of a spacetime where some physically relevant scalar quantity diverges. Recall that scalars are built from tensors in such a way that they are invariant under arbitrary coordinate transformations. So a physical singularity cannot be ‘‘transformed away’’. A famous example of such a singularity is $r = 0$ in the Schwarzschild spacetime. The scalar $R^{\mu\nu\sigma\rho} R_{\mu\nu\sigma\rho} \propto r^{-6}$ diverges at $r = 0$ and, consequently, the Schwarzschild spacetime loses its validity there.

3.2 The Field Equations

The *field equations* of General Relativity, sometimes also called *Einstein equations*, provide the link between the matter in the spacetime and its geometry, i.e. its metric:

$$R_{\mu\nu} - \frac{1}{2}g_{\mu\nu}R = 8\pi T_{\mu\nu}. \quad (3.3)$$

These are 16 coupled partial differential equations for the components $g_{\mu\nu}$ of the metric. The left-hand side contains the *Ricci tensor*

$$R_{\mu\nu} := R^{\sigma}{}_{\mu\sigma\nu},$$

and the *Ricci scalar*

$$R := R^{\sigma}{}_{\sigma}.$$

Both are formed by contracting the curvature tensor, which in turn is entirely determined by the metric and its first and second partial derivatives. So the left side of the field equations is a non-linear function of the metric components and its partial derivatives up to the second order. The right side of (3.3) contains the *energy-momentum tensor* $T_{\mu\nu}$ and a coupling constant whose exact value is explained later. The energy-momentum tensor acts as the source for the gravitation potentials $g_{\mu\nu}$. It is supposed to describe the distribution of energy and momentum of the matter in the spacetime. The construction of $T_{\mu\nu}$ is often based on intuition, but if the matter under consideration is governed by a Lagrangian, $T_{\mu\nu}$ can be derived in a definite way.

Since all the tensors involved are symmetrical, only 10 of the original 16 equations are actually independent. And since the Ricci tensor satisfies the contracted Bianchi identities

$$\left(R_{\mu\nu} - \frac{1}{2}g_{\mu\nu}R\right)^{;\nu} = 0, \quad (3.4)$$

the number of independent equations is reduced to 6, and we automatically get conservation laws for the energy-momentum tensor:

$$T_{\mu\nu}{}^{;\nu} = 0. \quad (3.5)$$

The 6 independent equations match the number of independent metric components: Of the original 16, symmetry accounts for 6. And the invariance of the field equations and all other relevant relations under general 4-dimensional coordinate transformations can be seen as a “gauge freedom”. Choosing a “gauge” leaves us with 6 independent components.

The conservation law (3.5) alone does not yield a conserved quantity in the usual sense since there is no natural way to integrate a tensor like $T_{\mu\nu}$. If the spacetime admits a Killing field ψ^μ , however, we find that

$$Q_\nu{}^{;\nu} := (T_{\mu\nu}\psi^\mu)^{;\nu} = T_{\mu\nu}{}^{;\nu}\psi^\mu + T_{\mu\nu}\psi^{\mu;\nu} = 0.$$

The first term vanishes due to (3.5), and the second term vanishes because $T_{\mu\nu}$ is symmetric whereas $\psi^{\mu;\nu}$ is antisymmetric since ψ^μ is a Killing field. The tensor Q_ν can now be interpreted as a conserved quantity with the help of Gauß' law:

$$\int_{\partial V} Q_\nu d\sigma^\nu = \int_V Q_\nu{}^{;\nu} dv = 0,$$

where V is some compact region of spacetime.

So where do the field equations (3.3) come from? They are an axiom. They cannot be derived from other principles, at least currently. There are, however, a couple of principles that motivate the form of the field equations.

- First and foremost, the field equations need to be equations for tensor components so that they are invariant under coordinate transformations, as required by the equivalence principle. Since we want to relate geometry to matter, we need to find suitable tensor expressions containing the metric on the one hand and tensor expressions describing the matter on the other.
- Then we demand that matter only enters the field equations via the energy-momentum tensor, so that different matter fields with the same distribution of energy and momentum yield the same geometry. The energy-momentum tensor should also be conserved automatically, which demands that something like the contracted Bianchi identities (3.4) holds.
- In the limit of weak gravitational fields, i.e. when the metric is just the Minkowski metric plus a perturbation, Newton's theory of gravity holds to a high degree of accuracy. So in this limit, we should recover Newton's theory of gravity from the field equations. This requirement fixes the coupling constant.
- And finally, we require that the field equations be of second order in g . That is, the field equations should not contain derivatives of the metric of order higher than 2. This requirement is based on the absence of third or higher derivatives in all the other basic physical laws.

Taken together, these principles can be shown¹ to fix the form of the field equations to be of the kind of (3.3). There is one important possibility to alter the field equations without violating any of the above requirements, however. Adding a term of the form $g_{\mu\nu}\Lambda$ —with $\Lambda \in \mathbb{R}$ being referred to as the *cosmological constant*—to the field equations (3.3), one gets

$$R_{\mu\nu} - \frac{1}{2}g_{\mu\nu}R = 8\pi T_{\mu\nu} + g_{\mu\nu}\Lambda.$$

This change does not violate any of the requirements because the metric is constant with respect to the covariant derivative: $g_{\mu\nu;\sigma} = 0$, which is another form of saying that the Levi-Civita connection of g is metric preserving.

¹See Hawking and Ellis (1973, pages 71ff.), for example.

This new term turns out to be useful to get models of our universe which are in agreement with experimental data. More concretely, Λ is thought of as providing the missing amount of energy that is needed to account for the behavior and form of our universe and for which there is no natural explanation yet. Due to this role, Λ is sometimes called “dark energy”.

4 Visualization Techniques

Visualization is the production of a pictorial representation of some abstract information. Its aim is to facilitate understanding of the depicted knowledge. In General Relativity, visualization tries to help getting an intuitive grasp of spacetimes and their features.

This is notoriously difficult due to spacetimes usually being four-dimensional. Our inability to visually process four-dimensional objects prevents us from depicting spacetimes directly. One simple way out of this is to use three-dimensional sections of spacetimes, where we hold one coordinate fixed at a specific value and examine the resulting three-dimensional hypersurface. For those three-dimensional objects, there are techniques to get good two-dimensional representations which can then be shown on a computer screen or printed to paper. A good overview of these techniques is given in Carlbom and Paciorek (1978). With some modern machinery like shutter glasses or polarized glasses and the corresponding projection apparatus, one can even avoid the need for a projection to two dimensions. Such setups are for example described in Bryson (1992) and on the site of the PORTAL¹ project.

In this work, we use the projection approach to create pictures of two- and three-dimensional features of spacetimes. In particular, we depict vector fields, hypersurfaces, the paths of geodesics, and light cones. These are, of course, not the only ways to visualize spacetimes: other prominent techniques include embedding diagrams of two-dimensional hypersurfaces² and Carter-Penrose diagrams³.

4.1 The Role of Coordinates

Without a coordinate representation of the metric, we cannot completely specify anything interesting like the geodesic equations or vector fields. But without a complete specification, we cannot visualize. Thus, most visualization techniques, and certainly those used here, require choosing a coordinate representation for the spacetime.

But in some cases, there is a discrepancy between the spacetime as a Lorentzian manifold and a particular coordinate representation of it. This frequently occurs when the chosen coordinates do not cover the whole manifold, producing the coordinate singularities described in the previous chapter.

In General Relativity, all relevant physical laws are invariant under general coordinate transformations. So in principle, all coordinate representations are on an equal footing.

¹<http://www.math.tu-berlin.de/portal/>

²For the theory of embedding diagrams, see Giblin (2004); Giblin, Marolf, and Garvey (2004); Jonsson (2001); Jonsson (2005). For applications to black hole spacetimes, see Davidson (2000); Frolov (2006); Hledík (2001); Kristiansson (1998); Giblin, Marolf, and Garvey (2004); Marolf (1999); Romano (1995).

³See Carter (1966) or Hawking and Ellis (1973, chapter 5).

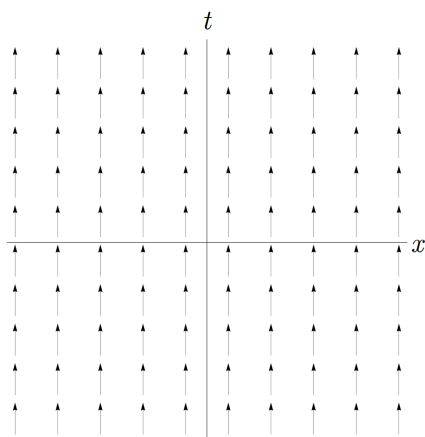


Figure 4.1: The vector field (4.1) in the coordinates $\{t, x, y, z\}$. The coordinates y and z are suppressed in the graphic.

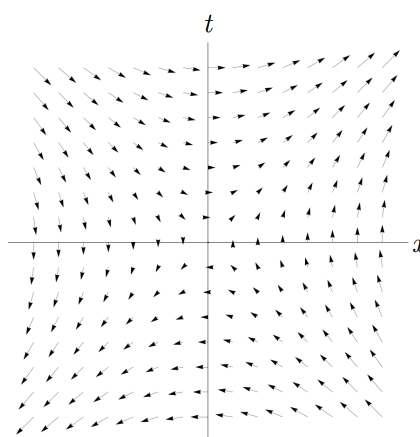


Figure 4.2: The vector field (4.2) in the coordinates $\{t, x, y, z\}$. The coordinates y and z are suppressed in the graphic.

But it is often the case that a specific set of coordinates is better suited than others for depicting some feature of a spacetime. For example, one coordinate system might make it obvious that a particular spacetime has certain symmetries whereas it might be very hard to see this for another coordinate system for the same spacetime.

4.2 Vector Fields and Hypersurfaces

Some basic features of a spacetime are often described in the form of vector fields. These might for example be Killing vector fields describing a direction of symmetry of the metric. Or they might be velocity vector fields or other vector fields associated with some curves in the spacetime.

A vector field $v \in \Gamma(TM)$ lives in the tangent bundle of the spacetime. To visualize it, we need the parameter representation of v with respect to a chosen chart (U, x) . The chart provides us with a basis $\{\partial_\mu\}$ of TM which can be used to obtain this parameter representation:

$$v = v^\mu \partial_\mu \quad \text{with } v^\mu \in C^\infty(M).$$

The $\{v_\mu\}$ can be combined with the chart map x to get maps $\{v_\mu \circ x\}$ which are functions of the coordinates $\{x_\mu\}$.

Take, for example, a spacetime with the coordinates (t, x, y, z) and the vector fields

$$\partial_t = (1, 0, 0, 0), \quad \text{and} \tag{4.1}$$

$$x \partial_t + t \partial_x = (x, t, 0, 0). \tag{4.2}$$

These two vector fields are shown in figures 4.1 and 4.2.

Another kind of structure that often arises when examining a spacetime is a hypersurface, i.e. a lower-dimensional subset of the spacetime. These might for example be

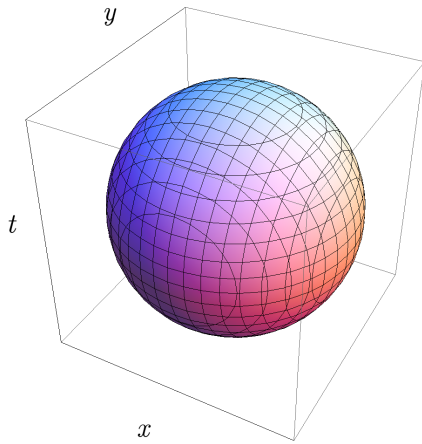


Figure 4.3: The hypersurface (4.3) in the coordinates $\{t, x, y, z\}$. The coordinate z is suppressed in the graphic. The lines on the surface denote the coordinate lines where all but one coordinate are hold fixed.

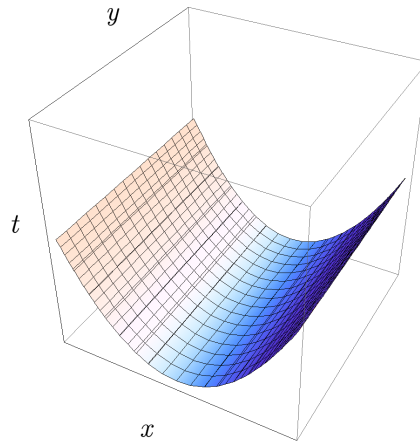


Figure 4.4: The hypersurface (4.4) in the coordinates $\{t, x, y, z\}$. The coordinate z is suppressed in the graphic. Note that the coordinate lines for y are straight, which is a manifestation of the absence of y from the defining equation of the hypersurface.

spacelike surfaces on which two events take place. Or the surface might represent the border between two regions of the spacetime with different properties.

Hypersurfaces are usually given in one of two forms: implicit or parametric. In implicit form, the hypersurface is given as an equation involving one or more of the coordinates. This equation removes one degree of freedom for the involved coordinates, and we thus get the lower-dimensional subset mentioned above. For a spacetime with coordinates (t, x, y, z) , examples for hypersurfaces given in implicit form might be

$$x^2 + y^2 + t^2 = 1, \quad \text{or} \quad (4.3)$$

$$x^2 - t = 1. \quad (4.4)$$

These two hypersurfaces are shown in figures 4.3 and 4.4.

The second representation of hypersurfaces is the parametric form in which the hypersurface is given as a function mapping one or more parameters to a point. Taken together, these points then make up the hypersurface. Two examples, the first one-dimensional and the second two-dimensional, are given by

$$f : [0, 4\pi] \rightarrow \mathbb{R}^4, \quad f(\tau) = \left(\cos \tau, \sin \tau, \frac{\tau}{10}, \text{const.} \right), \quad (4.5)$$

$$g : [-\pi, \pi] \times [-\pi, \pi] \rightarrow \mathbb{R}^4, \quad g(\tau_1, \tau_2) = \left(\tau_1, \tau_2, \frac{3}{2} \sin(\tau_1 \tau_2), \text{const.} \right). \quad (4.6)$$

Disregarding the last component, we can depict these surfaces as is done in figures 4.5 and 4.6.

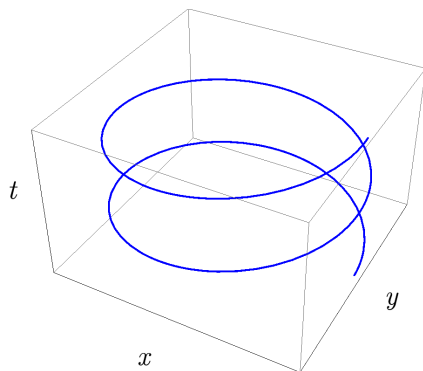


Figure 4.5: The hypersurface (4.5) with the last component suppressed.

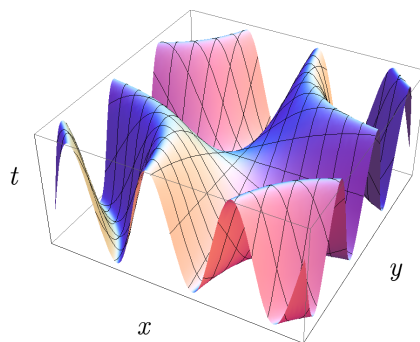


Figure 4.6: The hypersurface (4.6) with the last component suppressed.

4.3 Geodesics

Geodesics are curves γ that solve the geodesic equations, i.e. they represent the trajectories of freely falling particles. To completely determine γ , we need to specify initial conditions $\gamma(0)$ and $\gamma'(0)$. By choosing the length of the initial direction $\gamma'(0)$ appropriately, we can select the geodesics' type: $|\gamma'(0)| = 0$ for lightlike geodesics, $|\gamma'(0)| > 0$ for timelike geodesics. The result will then be a parametrized curve $\gamma : I \rightarrow M$ mapping some interval I to the spacetime M . So for the purpose of visualization, geodesics are one-dimensional hypersurfaces like those described in the previous section. Even though geodesics are a coordinate-invariant concept, the depicted curves will depend on the choice of coordinates since the initial conditions are specified with respect to the chosen chart.

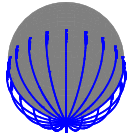
To get an overview of how the behavior of geodesics changes when the initial conditions are changed, it is insightful to depict multiple different geodesics at once. There are two basic ways to do this.

In the first, we let all geodesics originate from the same point but with different initial directions. Three examples of this procedure are shown in figure 4.7 for the Schwarzschild spacetime (3.2). In each of the three pictures, the initial directions are of the form

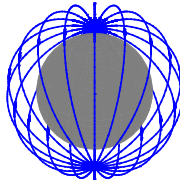
$$\psi \partial_t + \sin \alpha \partial_\theta + \cos \alpha \partial_\phi,$$

where α is chosen from $[0, 2\pi]$ in steps of $\pi/10$ and for each α value, ψ is determined such that the whole vector has zero length so that we get lightlike geodesics. The difference between the three pictures is the r value, the distance from the origin, of the initial position. From left to right, the distance increases from $2.5M$ via $3.0M$ to $4.0M$. In the first case the geodesics reach the horizon very soon, in the second case they enter orbits $r = \text{const}$ and are confined to them forever, and in the third case the geodesics recede to infinity.

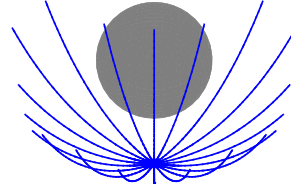
Another set of examples for plotting geodesics with the same origin but different initial directions is shown in figure 4.8. This time, only two coordinates (r, ϕ) are shown and



(a) Originating at $r = 2.5M$

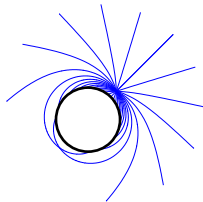


(b) Originating at $r = 3M$

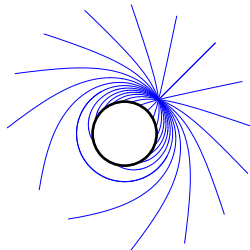


(c) Originating at $r = 4M$

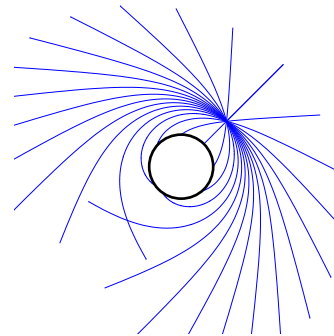
Figure 4.7: Three sets of geodesics in the Schwarzschild spacetime. Only the spatial components (r, θ, ϕ) are shown; the time t is suppressed. The dark sphere represents the event horizon $r = 2M$ of the body with mass M positioned at the origin.



(a) Originating at $r = 2.5M$



(b) Originating at $r = 3M$



(c) Originating at $r = 4M$

Figure 4.8: Three sets of geodesics in the Schwarzschild spacetime. Only the spatial components (r, ϕ) are shown; (t, θ) are suppressed. The dark circle represents the event horizon $r = 2M$ of the body with mass M positioned at the origin.

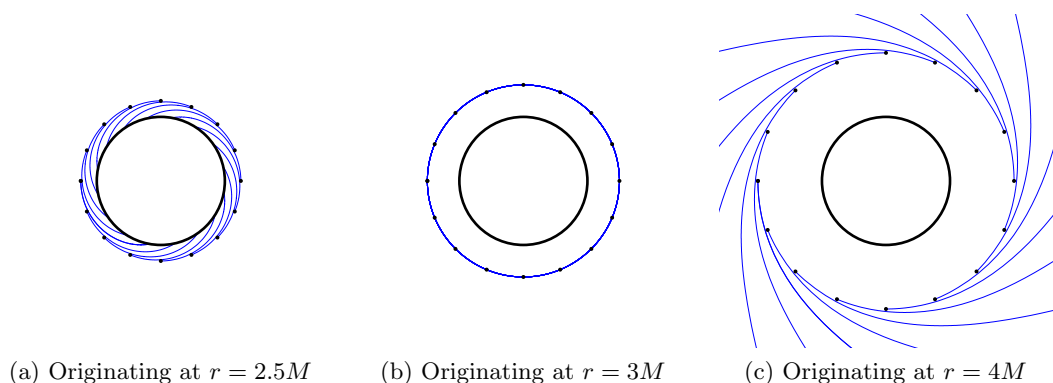


Figure 4.9: Three sets of geodesics in the (r, ϕ) plane of the Schwarzschild spacetime. In each graphic, the ϕ value of the initial position is varied from $-\pi$ to π whereas its r component takes a constant value. The initial direction is always $\psi \partial_t + \partial_\phi$.

the initial directions take the form

$$\psi \partial_t + \cos \alpha \partial_r + \sin \alpha \partial_\phi,$$

with α and ψ like above. So in contrast to the previous examples, the geodesics' initial directions now have a radial component. The initial positions are again chosen with different radial components r .

The second basic way to depict multiple geodesics is to let them start at different initial positions but with the same initial direction. Talking about the “same” initial directions, i.e. tangent vectors, at different points in the spacetime is just a heuristic, of course. Tangent vectors from different tangent spaces cannot be compared directly. What is meant here is that the parameter representation of the initial directions with respect to the chosen coordinate system is the same for all selected starting points.

An example will make this clearer. Consider again the Schwarzschild spacetime. Now we want to visualize geodesics whose initial directions are of the form

$$\psi \partial_t + \partial_\phi,$$

where, like above, ψ is always chosen so that the resulting vector is lightlike. We can plot those geodesics in the (r, ϕ) plane originating from points with varying ϕ values. In figure 4.9 this is done for three different values of r . The results are similar to those found in figure 4.7.

Another example is given by geodesics originating from points with varying r values and with initial directions of the form

$$\psi \partial_t \pm \partial_\phi.$$

This is done in figure 4.10 for $r \in [-10M, 10M]$.

We might want to do the same with the initial positions varying horizontally on a straight line that does not go through the origin, and with initial directions “pointing

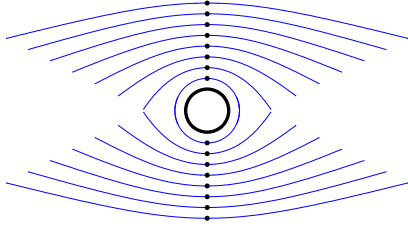


Figure 4.10: A set of geodesics in the Schwarzschild spacetime originating from points with different r values and with initial directions of the form $\psi \partial_t \pm \partial_\phi$. The (r, ϕ) plane is shown.

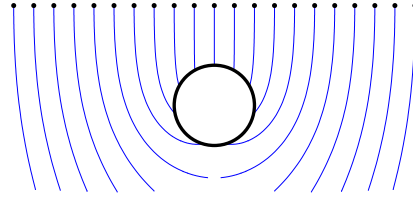


Figure 4.11: A set of geodesics in the (r, ϕ) plane of the Schwarzschild spacetime originating from points with different x values and with initial directions of the form $\psi \partial_t - \partial_y$.

down”. In other words, we want initial positions with varying x value and initial directions of the form $-\partial_y$. The Schwarzschild metric uses spherical coordinates, though, so in order to speak in terms of x and y we need to use the usual transformation laws

$$\begin{aligned} x &= r \cos \phi, & r &= \sqrt{x^2 + y^2}, \\ y &= r \sin \phi, & \phi &= \arctan\left(\frac{y}{x}\right). \end{aligned}$$

The initial direction then turns out to be

$$\psi \partial_t - \partial_y = \psi \partial_t - \sin \phi \partial_r - \frac{\cos \phi}{r} \partial_\phi.$$

The resulting geodesics are shown in figure 4.11 for $x \in [-10M, 10M]$.

4.4 Light Cones

When talking about light cones different people mean different things. One definition says that the future light cone of a point in a spacetime is the *boundary of the causal future* of that point. The causal future $J^+(p)$ of a point is the set of those points of the spacetime that can be reached by future-directed timelike or lightlike curves:

$$\begin{aligned} J^+(p) &:= \{q \in M \mid \exists \gamma : [0, 1] \rightarrow M \text{ future-directed timelike or lightlike} \\ &\quad \text{with } \gamma(0) = p \text{ and } \gamma(1) = q\}. \end{aligned}$$

So the future light cone $\widehat{C}^+(p)$ of a point $p \in M$ would be defined by:

$$\widehat{C}^+(p) := \partial J^+(p).$$

And similarly for the causal past $J^-(p)$ and the past light cone $\widehat{C}^-(p)$.

Another definition says that the future light cone of a point is the *causal future minus the chronological future* of that point:

$$\widetilde{C}^+(p) := J^+(p) \setminus I^+(p).$$

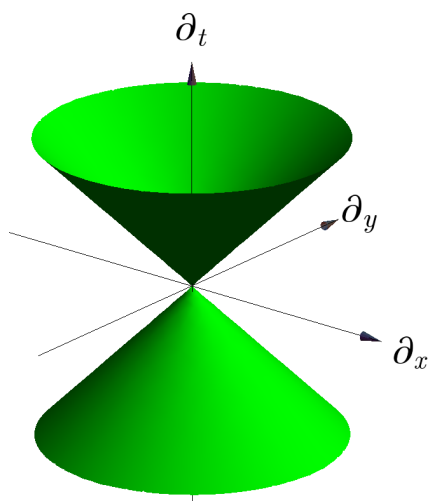


Figure 4.12: A light cone $C(p) \subset T_p M$ of Minkowski spacetime M . The coordinate z is suppressed.

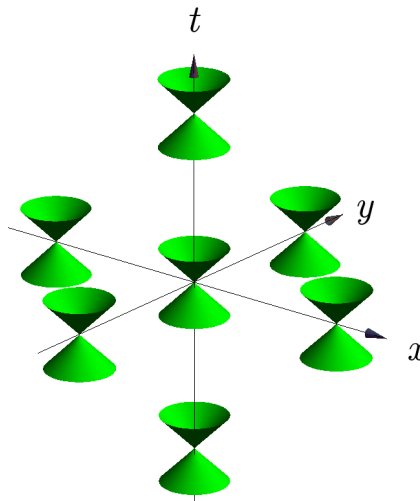


Figure 4.13: The light cones of multiple points in Minkowski spacetime. Since the Minkowski metric is the same at every spacetime point, the light cones do not change their form or orientation.

The chronological future $I^+(p)$ is defined very similarly to the causal future:

$$I^+(p) := \{q \in M \mid \exists \gamma : [0, 1] \rightarrow M \text{ future-directed timelike} \\ \text{with } \gamma(0) = p \text{ and } \gamma(1) = q\}.$$

These two definitions for light cones are equivalent when, colloquially speaking, no points are missing from the spacetime in question.⁴ Both definitions have in common that they define light cones to be subsets of the spacetime.

The most common definition for light cones, however, puts them into the tangent space of a point⁵:

$$C(p) := \{v \in T_p M \mid g(v, v) = 0\}.$$

That is, the light cone $C(p)$ of a point is the set of all tangent vectors at that point with vanishing length. We will use this definition of the light cone since it is comparatively easy to handle computationally. As we discussed in section 2.1.5, especially figure 2.7, the defining equation $g(v, v) = 0$ yields a hypersurface in the tangent space. For the Minkowski spacetime (3.1), the light cone $C(p)$ of any point is a perfect double cone which, upon suppressing one of the spatial coordinates, can be visualized: see figure 4.12.

It is important to keep in mind that $C(p) \subset T_p M$. For the purpose of visualization, however, it is useful to have structures that live directly in M . One way of getting such

⁴See Hawking and Ellis (1973, pages 182ff.) for details.

⁵This definition is used by Hawking and Ellis (1973); Beem, Ehrlich, and Easley (1996); Misner, Thorne, and Wheeler (1973); O'Neill (1983); Sachs and Wu (1977).

a structure from a light cone is the *exponential map*:

$$\begin{aligned}\exp_p &: T_p M \rightarrow M, \\ \exp_p(v) &= \gamma_{p,v}(1),\end{aligned}$$

where $\gamma_{p,v}$ is the unique geodesic curve with $\gamma_{p,v}(0) = p$ and $\gamma'_{p,v}(0) = v$. Note that \exp_p might not be defined for every $v \in T_p M$ since $\gamma_{p,v}(1)$ may not be defined. But it can be shown⁶ that for every point $p \in M$ there is a neighborhood $U \subset T_p M$ of $0_p \in T_p M$ where \exp_p is not only defined but is even smooth and has a smooth inverse. Due to the way we defined \exp_p , the image $\exp_p(C_p)$ of the light cone at p will be a circular section of

$$\tilde{C}(p) := \tilde{C}^+(p) \cup \tilde{C}^-(p),$$

which is the set of points traced out by all lightlike geodesics originating at p . To get the whole set, we need to scale the parameter range of the geodesic in the definition of \exp_p . This amounts to considering the set

$$\{v \in C(p), t \in \mathbb{R} \mid \exp_p(tv)\}. \quad (4.7)$$

Note that scaling a lightlike vector v like this does not change its lightlike character. When we restrict our view to the region U where \exp_p is well-mannered, (4.7) is identical to $\tilde{C}(p)$.⁷

So in this way \exp_p provides us with the means to map $C(p)$ to the corresponding structure in the spacetime. What we will do for visualizing light cones *in the spacetime* is to simply depict $C(p)$ and think of it as “modulo $\exp(p)$ ”. In other words, this means that we will regard $C(p)$ as a linear approximation to $\tilde{C}(p)$. This resembles the way that $T_p M$ is a linear approximation to M at the point p (see section 2.1.2).

This approach was used in figure 4.13 to show the light cones of multiple points in the Minkowski spacetime (3.1), drawn at their respective base point. Figure 4.14 gives some visual justification for the technique: the shown lightlike geodesics lie exactly on the light cone. This exactness of the approximation is of course due to the simplicity of Minkowski spacetime. When we depict a combination of lightlike geodesics and light cones in the Schwarzschild spacetime (3.2) for example, as is done figure 4.15, we see that after a while the geodesics cease to lie on the light cone.

Depicting multiple light cones at their respective base point is a useful way to investigate the causal structure of a spacetime. Consider for example figure 4.16a which shows a few light cones in the Schwarzschild spacetime. Outside the event horizon $r = 2M$ the light cones are upright which means that ∂_t is timelike there. But as one crosses the horizon, the light cones abruptly tip over so that ∂_t becomes spacelike and ∂_r takes its place as a timelike vector field. That the change happens so suddenly is due the choice of coordinates, just like the coordinate singularity at the horizon. A better set of coordinates

⁶See O’Neill (1983, pages 70ff.), for example.

⁷See Hawking and Ellis (1973, page 184).

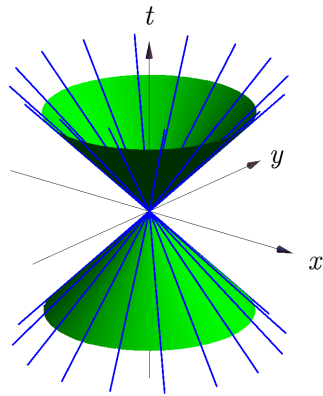


Figure 4.14: The light cone at some point p in Minkowski spacetime, together with some lightlike geodesics emanating from p . The geodesics lie on the light cone.

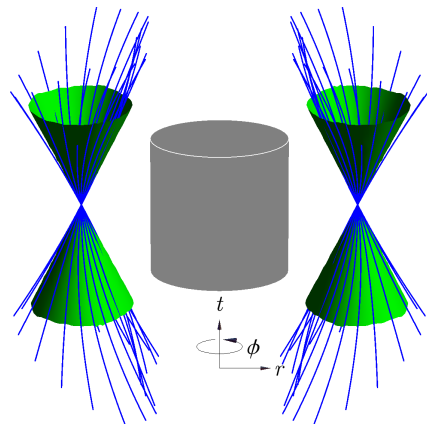


Figure 4.15: Two sets of geodesics and the corresponding light cones in the Schwarzschild spacetime. The dark cylinder represents a segment of the event horizon. The geodesics cease to lie on the light cone after a while.

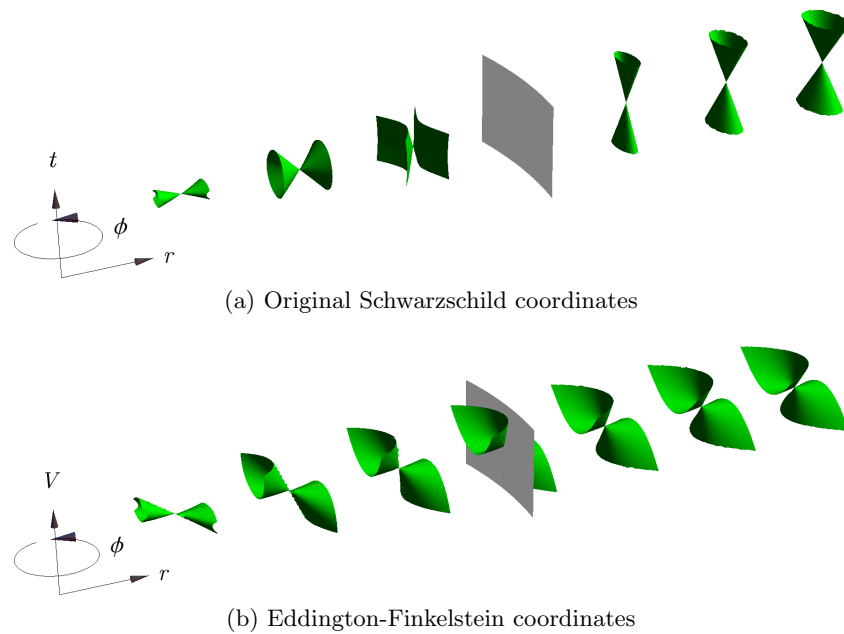


Figure 4.16: Light cones in the Schwarzschild spacetime in the original coordinates and in Eddington-Finkelstein coordinates. In both cases, the light cones tip over when crossing the event horizon $r = 2M$ (indicated by the dark plane).

in this case are given by the *Eddington-Finkelstein coordinates* (V, r, θ, ϕ) where V is defined by

$$V := t + \int \frac{1}{1 - 2m/r} dr.$$

The Schwarzschild metric now reads

$$ds^2 = \left(1 - \frac{2m}{r}\right) dV^2 - 2 dV dr - r^2 (d\theta^2 + \sin^2 \theta d\phi^2). \quad (4.8)$$

These coordinates are adapted to radially ingoing lightlike geodesics since they are given by $V = \text{const}$. Figure 4.16b shows the situation in Eddington-Finkelstein coordinates. Now the light cones do not tip over suddenly anymore but do so smoothly. This tipping signifies the fate of radially outgoing lightlike geodesics: for $r > 2M$ they can escape, at the event horizon $r = 2M$ they are confined to fixed orbits, and for $r < 2M$ they are forced into the real singularity $r = 0$ with no chance of escaping.

5 Implementation

5.1 The Computer Algebra System Mathematica

Mathematica is a non-free software system of a kind generally referred to as computer algebra systems which allow doing “mathematical experimentation”. Its main strength is that it makes it possible to do symbolic calculations on the computer: differentiate and integrate functions; solve algebraic, differential, and difference equations; simplify expressions. Mathematica is also able to do all of those actions numerically which is useful if, for example, a problem cannot be tackled symbolically or if one is interested in the numerical solution only. Another important capability is visualization. Mathematica can create all kinds of two- and three-dimensional plots of discrete data, arbitrary functions, or vector fields using lines, surfaces, contours, or arrows for display. And finally, Mathematica provides a powerful programming language that can be used to extend existing and write new features.

There are quite a few alternative software systems with similar capabilities: the non-free Maple and Matlab; and the free Maxima, Octave, Scilab, and Sage. Mathematica was chosen for this work partly due to its easy availability on the campus network and the author’s previous experience with it. But the main reason for the choice was the elegant, expressive, and concise programming language provided by Mathematica. The following table lists all the mentioned computer algebra systems again together with their web address.

Mathematica	http://www.wolfram.com/products/mathematica/
Maple	http://www.maplesoft.com/Products/Maple/
Matlab	http://www.mathworks.de/products/matlab/
Maxima	http://maxima.sourceforge.net/
Octave	http://www.gnu.org/software/octave/
Scilab	http://www.scilab.org/
Sage	http://www.sagemath.org/

5.2 The GeodesicGeometry Package

To make it easy to apply the visualization techniques described in the previous chapter to various spacetimes, the Mathematica package `GeodesicGeometry`¹ bundles all the necessary functionality. It provides an object-oriented interface with a constructor `GeodesicGeometry` that is called with information about the metric of the spacetime as

¹The `GeodesicGeometry` package is freely available from <http://www.math.tu-berlin.de/~schoenf/GeodesicGeometry/>.

arguments. It returns an object encapsulating this information for later use. For example, to create an object for the Schwarzschild spacetime, we can use the following:

```
Needs["GeodesicGeometry`"]
m = 1;
schwarzschild = GeodesicGeometry[
  {t, r, Theta, Phi},
  {dt, dr, dTheta, dPhi},
  (1 - 2 m/r) dt^2 - 1/(1 - 2 m/r) dr^2 -
  r^2 (dTheta^2 + Sin[Theta]^2 dPhi^2)];
```

This loads the `GeodesicGeometry` package with the built-in function `Needs` and then calls the constructor `GeodesicGeometry` with three arguments: a list of the names of the coordinates we want to use, a list of the names of their differentials, and the line element ds^2 of the spacetime in these coordinates. Internally, the constructor `GeodesicGeometry` mainly computes the inverse metric and the Christoffel symbols and stores them in the returned object for later use so that they do not have to be computed over and over again. This results in an object `schwarzschild` that can be passed to the other functions provided by this package. These functions are described in the following sections.

5.3 Solving the Geodesic Equations Numerically

With the metric and thus the inverse metric and the Christoffel symbols given, the geodesic equations (2.12) are four coupled ordinary differential equations of second order for the four unknown components γ^μ of the geodesic. So a unique solution exists if we specify the initial positions $\gamma^\mu(0)$ and the initial velocities $\gamma^{\mu'}(0)$. Nonetheless, it is often very difficult to find the solution analytically. Even if it is possible, Mathematica's command for solving differential equations analytically, `DSolve`, might take a very long time to do so.

We do not need the analytic expression for the geodesics for plotting them, numerical approximations suffice. Thus, `GeodesicGeometry` uses Mathematica's numerical solver for differential equations, `NDSolve`, to find these numerical approximations. There are various methods for solving ordinary differential equations, most of which deal with initial value problems for ordinary differential equations that are posed in the following form:

$$\mathbf{y}'(\tau) = \mathbf{f}(\tau, \mathbf{y}), \quad \mathbf{y}(0) = \boldsymbol{\alpha}, \quad (5.1)$$

where \mathbf{y} is the dependent variable that we are trying to find, \mathbf{f} is some well-mannered function, and $\boldsymbol{\alpha}$ is the initial value. All of these are vector-valued, so (5.1) describes a system of ordinary differential equations of first order. Any system of ordinary differential equations of higher order can be reformulated as a system of equations of first order by considering the derivatives of the dependent variable as new dependent variables.

The simplest numerical method for solving these kinds of systems is called the *explicit Euler method*. First create a discrete mesh for the parameter τ :

$$\tau_0 = 0, \quad \tau_r = \tau_0 + rh \quad \text{for } r = 1, 2, \dots,$$

and where h is the *step length*. Then consider the Taylor expansion of $\mathbf{y}(\tau_r + h)$ about τ_r :

$$\mathbf{y}(\tau_r + h) = \mathbf{y}(\tau_r) + h\mathbf{y}'(\tau_r) + \mathcal{O}(h^2).$$

As an approximation for $\mathbf{y}(\tau_r)$, the explicit Euler method then computes the value \mathbf{Y}_r at step r by simply using only the first two terms of the expansion:

$$\mathbf{Y}_{r+1} = \mathbf{Y}_r + h\mathbf{f}(\tau_r, \mathbf{Y}_r).$$

This is a so-called single-step iterative approach because it computes \mathbf{Y}_1 from $\mathbf{Y}_0 = \boldsymbol{\alpha}$, \mathbf{Y}_2 from \mathbf{Y}_1 , and so on. An approximation curve \mathbf{Y} can then be obtained by fitting an interpolating function to the computed points \mathbf{Y}_r . There are, of course, more advanced techniques for solving ordinary differential equations, many of which are described in Fox and Mayers (1988). Mathematica's *NDSolve* uses one of those more advanced algorithms.²

GeodesicGeometry offers the function *SolveGeodesicEquations* as a convenient wrapper around *NDSolve* adapted to finding solutions of the geodesic equations. It is passed the spacetime object, the initial conditions, and the desired parameter range. For example, if we want to find the geodesic originating at $(t = 0, r = 4m, \theta = \pi/2, \phi = 0)$ with initial direction $2\partial_t + \partial_r$, we can use:

```
SolveGeodesicEquations[
  schwarzschild,
  {0, 4 m, Pi/2, 0}, {2, 1, 0, 0},
  {0, 1}]
```

This will result in four interpolating functions for the four components of the geodesic.

When the spacetime has singularities, *SolveGeodesicEquations* might yield unreasonable results when the solution gets close to one. To avoid this, *SetSingularityCriterion* can be used to instruct GeodesicGeometry to stop computations when reaching a singularity. It takes the spacetime object and a list of functions which can signal that a singularity has been reached by returning a true value. For the Schwarzschild spacetime, this might look like this:

```
SetSingularityCriterion[
  schwarzschild,
  {Abs[r[#] - 2 m] < 10-3},
  Abs[r[#] - 0 m] < 10-3}&]
```

5.4 Plotting Geodesics

To more conveniently plot a set of geodesics, GeodesicGeometry offers functions to do that for sets of null or timelike geodesics. When specifying the initial directions of the set of geodesics we want to visualize, we need to make sure that their length

²See <http://documents.wolfram.com/mathematica/book/section-A.9.4> for information about the algorithms used, and see <http://reference.wolfram.com/mathematica/tutorial/NDSolveOverview.html> for more information on *NDSolve*.

always matches the desired value, i.e. zero for lightlike geodesics and some positive constant for timelike geodesics. This quickly becomes bothersome to ensure manually, so GeodesicGeometry let's you specify so-called *initial direction templates* which contain one unknown variable whose value is automatically determined so that the resulting vector's length is what is desired. Whereas a normal vector is represented as a simple tuple like $\{0, 4m, \pi/2, 0\}$, a vector template looks like $\{\text{Psi}, \{0, \text{Psi}, \pi/2, 0\}\}$. The unknown Psi is then automatically determined so that the resulting vector has the desired length at the current spacetime point. This approach generally yields two vectors since the equation for Psi is quadratic. When Psi is used as the time component, the resulting vectors will be the future- and past-directed solutions.

As described in the previous chapter, there are two basic methods for plotting sets of geodesics: sprays and bundles. To plot sprays, GeodesicGeometry offers *PlotNullSpray* and *PlotTimelikeSpray*. Both take the spacetime object, an initial position, and a set of initial direction templates. Additional optional arguments determine the desired range of the geodesics, the coordinates that should be plotted, and the coordinate transformation that should be applied for plotting. To plot bundles, *PlotNullBundle* and *PlotTimelikeBundle* can be used. They take the spacetime object, a set of initial positions, and an initial direction template. The optional arguments are the same as for the spray variants. The functions *PlotTimelikeSpray* and *PlotTimelikeBundle* for timelike geodesics determine initial directions such that they have unit length. This indirectly fixes the assumed signature of the specified line element to be $(+, -, -, -)$. If only lightlike geodesics are plotted, the signature does not matter.

In both cases, the resulting set of solutions to the geodesic equations will look like $\{\{\gamma_{11}, \gamma_{12}\}, \{\gamma_{21}, \gamma_{22}\}, \dots\}$, where γ_{1i} are the two solutions for the first tuple of initial position and initial direction template, γ_{2i} the second, and so on. There are two solutions for every such tuple since an initial direction template generally yields two vectors, as explained above. To get meaningful pictures, we have to reorder the solutions a bit so that those coming from the same kind of initial direction are in the same set. For example, if the unknown variable in the initial direction template is used for the time component, we want all future-directed solutions in one set and all past-directed solutions in the other. This reordering leads to the two sets $\{\gamma_{11}, \gamma_{21}, \dots\}$ and $\{\gamma_{12}, \gamma_{22}, \dots\}$. These can now be plotted by choosing the desired components from each solution, applying the specified coordinate transformation, and using Mathematica's *ParametricPlot* or *ParametricPlot3D*.

Using *PlotNullSpray* for the Schwarzschild spacetime to plot geodesics emanating from $(0, 4m, \pi/2, 0)$ with initial directions of the form $\psi\partial_t + \cos v\partial_r + \sin v\partial_\phi$ and showing (r, ϕ, t) as cylindrical coordinates is demonstrated in figure 5.1. A similar invocation of *PlotNullBundle*, this time with (r, ϕ) as polar coordinates, is shown in figure 5.2.

5.5 Plotting Light Cones

For plotting light cones, GeodesicGeometry offers the function *PlotNullCone*. Its arguments are the spacetime object, a position, and, optionally, the plot coordinates,

```
Needs["VectorAnalysis`"];
PlotNullSpray[
  schwarzschild,
  {0, 4 m, Pi/2, 0},
  Table[{Psi, {Psi, Cos[v], 0, Sin[v]}}, {v, 0, 2 Pi, Pi/10}],
  ParameterRange -> {0, 1},
  PlotCoordinates -> {r, Phi, t},
  PlotCoordinateTransformation ->
  (CoordinatesToCartesian[#, Cylindrical]&)]
```

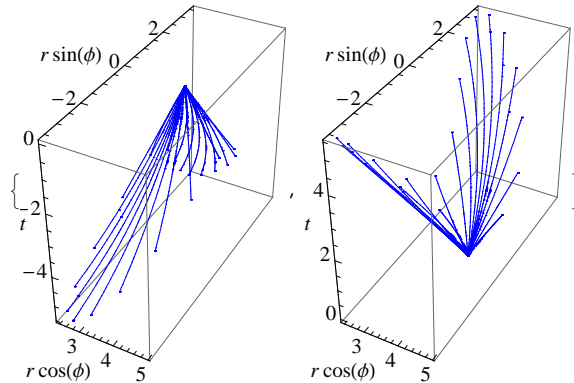


Figure 5.1: An invocation and the results of *PlotNullSpray* for the Schwarzschild spacetime. The plot on the left side shows the past-directed geodesics while the plot on the right shows the future-directed ones.

```
PlotNullBundle[
  schwarzschild,
  Table[{0, 4 m, Pi/2, v}, {v, 0, 2 Pi, Pi/10}],
  {Psi, {1, 0, 0, Psi}},
  ParameterRange -> {0, 10},
  PlotCoordinates -> {r, Phi},
  PlotCoordinateTransformation ->
  ({#1[[1]] Cos[#1[[2]]], #1[[1]] Sin[#1[[2]]}]&)]
```

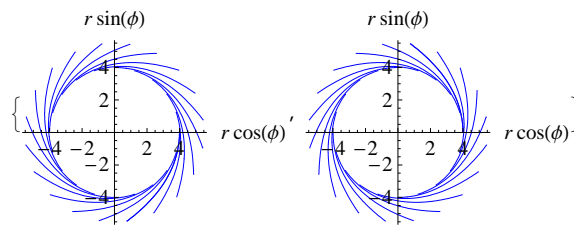


Figure 5.2: An invocation and the results of *PlotNullBundle* for the Schwarzschild spacetime. The two plots show geodesics starting from the same set of points but with opposite initial directions.

```
PlotNullCone[
  schwarzschild,
  {0, 4 m, Pi/2, Pi/2},
  PlotCoordinates -> {r, t},
  SolveCoordinate -> t,
  PlotRangeOffsets -> 1]
```

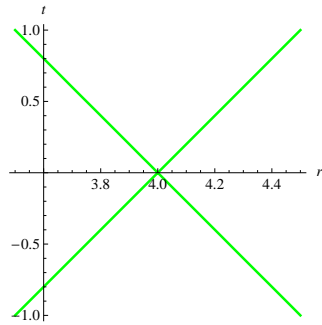


Figure 5.3: An invocation and the result of *PlotNullCone* for the Schwarzschild spacetime and with the coordinates r and t .

```
PlotNullCone[
  schwarzschild,
  {0, 4 m, Pi/2, Pi/2},
  PlotCoordinates -> {r, Phi, t},
  SolveCoordinate -> t,
  PlotRangeOffsets -> 1,
  PlotCoordinateSystem ->
  Cylindrical]
```

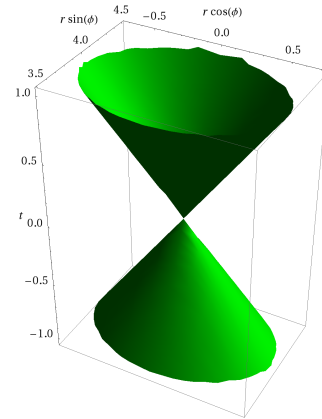


Figure 5.4: An invocation and the result of *PlotNullCone* for the Schwarzschild spacetime and with the cylindrical coordinates r , ϕ , and t .

the range of those plot coordinates, and the coordinate system that should be used for plotting.

Internally, *PlotNullCone* basically solves $g_p(v, v) = 0$ for one component v_i of $v = (v_0, v_1, v_2, v_3)$. Thus v_i becomes a function of the other components. Which of the components is solved for can be specified and the quality of the resulting plot often depends on the choice. From the resulting tuple, *PlotNullCone* then picks the wanted components and plots them as a parametric surface, respecting the given plot ranges and coordinate system. If three plot components are specified, the result will be a 3D plot of a two-parameter surface. For two plot components, it will be a 2D plot of a one-parameter surface, i.e. a curve. The possibility of applying arbitrary coordinate transformations is the reason that *PlotNullCone* uses *ParametricPlot* and *ParametricPlot3D* rather than *ContourPlot* and *ContourPlot3D*, even if the latter would automatically take care of choosing the best component to solve the equation for.

Figures 5.3 and 5.4 show example applications of *PlotNullCone* for the Schwarzschild spacetime.

6 Application to Particular Spacetimes

6.1 Gödel's Spacetime

Gödel (1949) describes a spacetime with remarkable properties. It has a five-dimensional group of isometries making it completely homogeneous (i.e. stationary and spatially homogeneous). It solves the field equations for a pressure-free perfect fluid with negative cosmological constant. And even though topologically it is just \mathbb{R}^4 , it allows closed timelike curves through every point.

The spacetime's line element is given by

$$\begin{aligned} ds^2 &= (dt + e^x dy)^2 - dx^2 - \frac{e^{2x}}{2} dy^2 - dz^2 \\ &= dt^2 - dx^2 + \frac{e^{2x}}{2} dy^2 - dz^2 + 2e^x dt dy. \end{aligned} \tag{6.1}$$

This form makes it apparent that there are three trivial Killing fields: ∂_t , ∂_y , and ∂_z . A fourth one is given by the line element's symmetry under the transformation $x \rightarrow x + a$, $y \rightarrow e^{-a}y$ which yields $\partial_x - y\partial_y$. These four account for the homogeneity of the spacetime. It is also easy to verify that (6.1) satisfies the field equations (3.3) for $\Lambda = -1$ and $T_{\mu\nu} = u_\mu u_\nu$, where $u^\mu = (2\sqrt{2\pi})^{-1} \partial_t$ can thus be interpreted as the world lines of the fluid.

To examine the behavior of light, we need to solve the geodesic equations (2.12). As Kundt (1956) and Chandrasekhar and Wright (1961) show, this can be done analytically for the Gödel spacetime. For our purposes, however, it suffices to obtain numerical solutions as described in the previous chapter. Figure 6.1 shows a set of geodesics starting from the origin with initial directions of the form

$$\psi \partial_t + \cos \alpha \partial_x + \sin \alpha \partial_y \tag{6.2}$$

where $\alpha \in [0, 2\pi]$ and, as usual, ψ is chosen such that the resulting geodesic is lightlike for every α . The mostly irrelevant coordinate z has been suppressed and projections to three coordinate planes have been added. Initially, the geodesics move "outwards", but after a finite parameter time they reach a turning point and refocus on a point on the t axis. After reaching this point, the geodesics repeat their behavior leading to a periodic appearance. Timelike geodesics behave similarly: figure 6.2 shows a set of geodesics with tangent vectors of unit length (in red) in conjunction with the geodesics from the previous figure (in blue).

Since ∂_t , ∂_y , and ∂_z are Killing fields, the behavior of the geodesics does not change when moving along those directions. It does change, however, when we use different

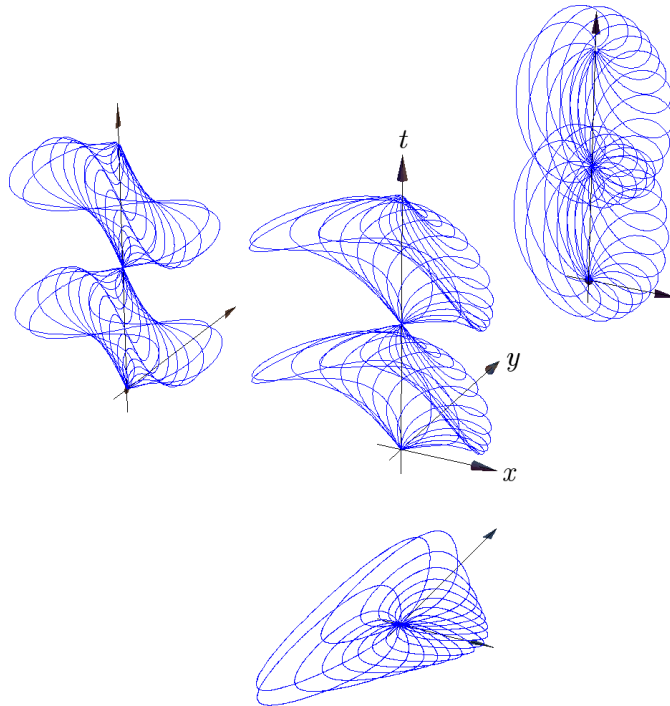


Figure 6.1: A set of geodesics starting from the origin with initial directions of the form $\psi\partial_t + \cos\alpha\partial_x + \sin\alpha\partial_y$. The mostly irrelevant coordinate z has been suppressed and projections to three coordinate planes have been added.

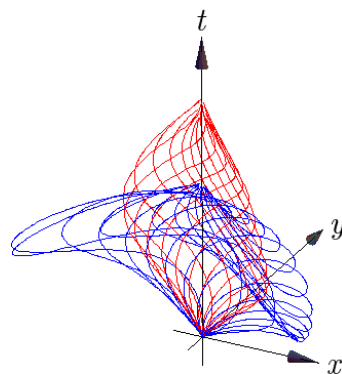


Figure 6.2: Two sets of geodesics starting from the origin, one consisting of lightlike geodesics (in blue) and the other consisting of timelike geodesics (in red).

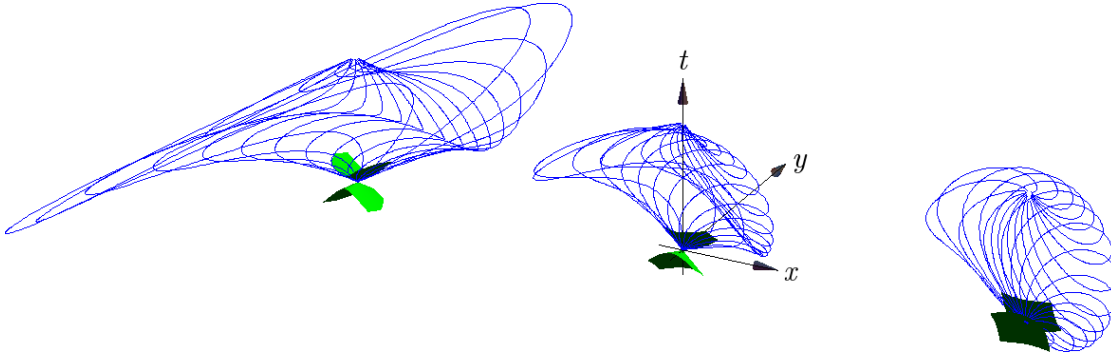


Figure 6.3: Three sets of geodesics originating from points with different initial x values x_0 . The sets tip over as one moves from smaller to larger x_0 values (from left to right). The separation of the three sets on the x axis is not to scale: they are depicted farther apart than they actually are because the plots would overlap otherwise.

initial x coordinate values x_0 : this is depicted in figure 6.3. The existence of a horizon and the refocusing are not affected. But in order to obtain a representative sample of geodesics at each starting point, the initial directions have to be adjusted. Instead of always using (6.2), we now need to scale the amplitude of the ∂_y component:

$$\psi \partial_t + \cos \alpha \partial_x + 3^{-x_0} \sin \alpha \partial_y.$$

The maximum distance travelled in the ∂_y direction thus becomes smaller when moving from smaller to larger x_0 values. But independently of this effect, the sets of geodesic also seem to “tip over” when moving from smaller to larger x_0 values. The light cones shown at the respective base points of the geodesics provide a good indication for this.

The tipping over of the light cones means that ∂_y becomes timelike when moving from smaller to larger x_0 values. But in addition to tipping over, the light cones also “open up” so that ∂_t always stays timelike as it should since the world lines of the matter are a multiple of it. These are the key ingredients that allow the formation of closed timelike curves¹, an example of which is depicted in figure 6.4.

Most of the mentioned properties of Gödel’s spacetime can be better visualized when using the cylindrical form of the line element. It is obtained from the original line element (6.1) by the following transformation:

$$\begin{aligned} e^x &= \cosh(2r) + \cos(\phi) \sinh(2r), \\ y e^x &= \sqrt{2} \sin(\phi) \sinh(2r), \\ \tan\left(\frac{\phi}{2} + \frac{t - 2u}{2\sqrt{2}}\right) &= e^{-2r} \tan\left(\frac{\phi}{2}\right), \\ z &= 2w. \end{aligned} \tag{6.3}$$

¹For more on closed timelike curves in the Gödel spacetime and their implications, see Bell (2002); Malament (1984); Pfarr (1981); Rosa and Letelier (2007); Stein (1970).

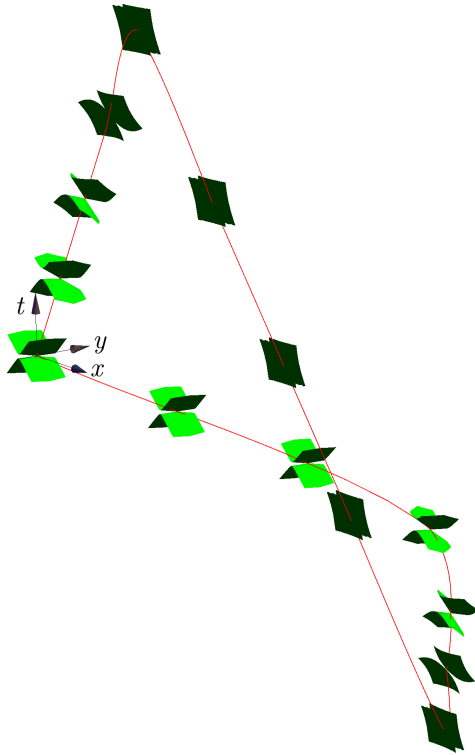


Figure 6.4: Recipe for constructing a closed timelike curve in the Cartesian frame of the Gödel spacetime. Start from $x = -2$. Then move along ∂_t and ∂_x until the light cones tip over sufficiently. Then move along $-\partial_t$ and ∂_y as far as necessary. Then go back to the origin.

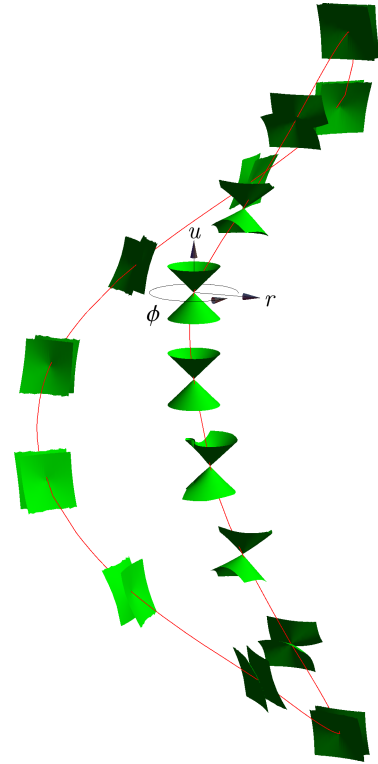


Figure 6.5: Recipe for constructing a closed timelike curve in the cylindrical frame of the Gödel spacetime. Start at the origin. Then move along ∂_u and ∂_r until the light cones tip over sufficiently. Then spiral back along ∂_ϕ and $-\partial_u$. Then go back to the origin.

This system of equations is rather complicated to handle, and Gödel (1949) is very terse in describing its derivation. But Stein (1970) argues that the transformation is well-defined and meaningful. Most importantly, we can solve it for the old coordinates (t, x, y, z) :

$$\begin{aligned} t &= 2s - \sqrt{2}\phi + 2\sqrt{2} \arctan\left(e^{-2r} \tan \frac{\phi}{2}\right), \\ x &= \log \cosh 2r + \cos \phi \sinh 2r, \\ y &= \frac{\sqrt{2} \sin \phi \sinh 2r}{\cosh 2r + \cos \phi \sinh 2r}, \\ z &= 2w. \end{aligned}$$

Thus we can transform the line element to the new coordinates (u, r, ϕ, w) :

$$\begin{aligned} ds^2 &= \left(du + \sqrt{2} \sinh^2 r d\phi\right)^2 - dr^2 - (\sinh^4 r + \sinh^2 r) d\phi^2 - dw^2 \\ &= du^2 - dr^2 - dw^2 + (\sinh^4(r) - \sinh^2(r)) d\phi^2 + 2\sqrt{2} \sinh^2(r) d\phi du. \end{aligned}$$

Due to the transformation, ϕ is a cyclic coordinate with period 2π and r is interpreted as a radial coordinate. The world lines of matter are now u lines. The line element's components do not depend on ϕ , so ∂_ϕ is a Killing field. It turns out that it is independent from the others so it is the fifth Killing field, describing the spacetime's rotational symmetry. It does not seem to be possible to solve the transformation (6.3) for the new coordinates, so it is not easily possible to find the representation of a vector field like ∂_ϕ in the old coordinates. For this particular case, however, the representation can be found with a bit of experimentation. It turns out to be

$$\sqrt{2} \partial_\phi = 2(1 + e^{-x}) \partial_t - y \partial_x + \left(\frac{1}{2}y^2 - e^{-2x} - 1\right) \partial_y.$$

The behavior of geodesics and light cones in the cylindrical frame of the Gödel spacetime can be succinctly represented in a plot which was first used in Hawking and Ellis (1973) and the crucial parts of which are shown in figure 6.6. The light cones tip over as one moves radially outwards so that ∂_ϕ becomes timelike eventually, and the geodesics have a horizon and refocus. The original picture purports to let the geodesics start at the origin which means from $r = 0$ in particular. This presents a technical difficulty since the line element is singular there. In figure 6.6, $r = 10^{-5}$ is used instead. Also, the initial velocity templates need to be adapted to the starting position again so that a representative sample of geodesics is computed:

$$\psi \partial_u + \cos \alpha \partial_r + 10^5 \sin \alpha \partial_\phi.$$

As figure 6.7 shows, the geodesics also tip over like the light cones. Just like in the Cartesian frame, these ingredients can be used to construct closed timelike curves through any point. An example is shown in figure 6.5.

For more visualization work on the Gödel spacetime, see Andréka et al. (2008) and Sahdev, Sundararaman, and Modgil (2006).

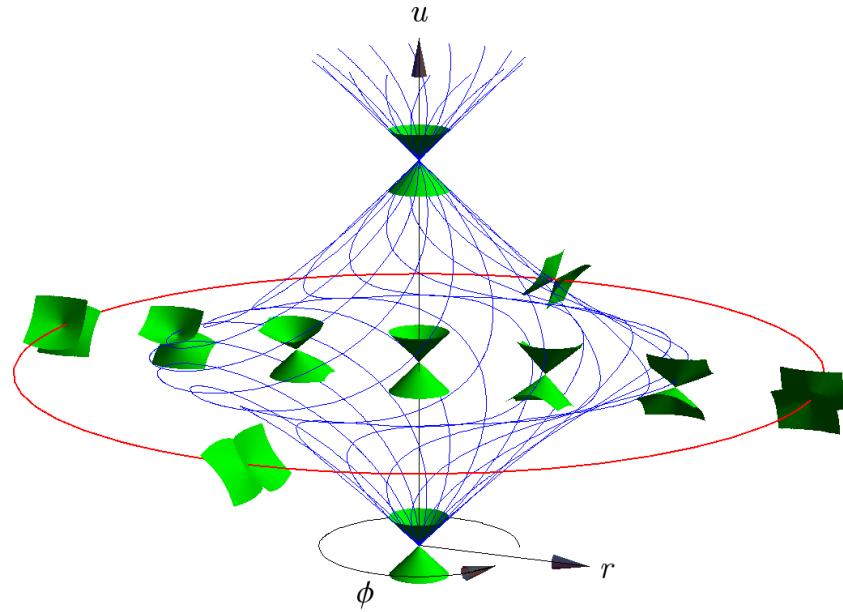


Figure 6.6: A set of geodesics, a few light cones, and a closed timelike curve in the cylindrical frame of the Gödel spacetime. The geodesics have a horizon and refocus. The light cones tip over as one moves radially outwards so that ∂_ϕ becomes timelike eventually and thus forms a closed timelike curve.

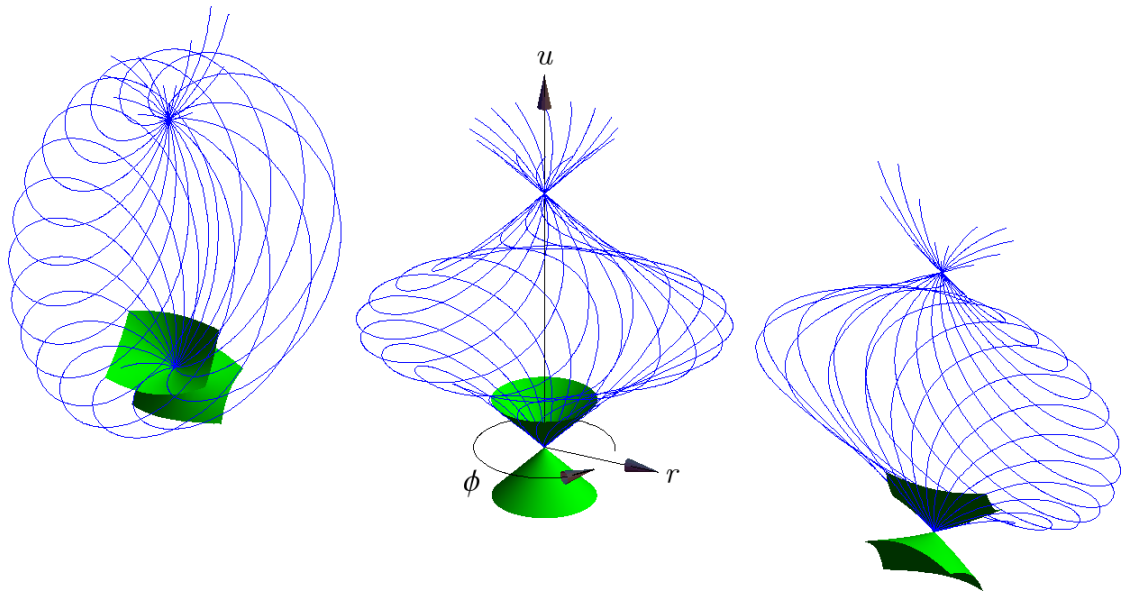


Figure 6.7: Three sets of geodesics in the cylindrical frame of the Gödel spacetime. The sets tip over like the light cones. The radial separation of the three sets is not to scale: they are depicted farther apart than they actually are because the plots would overlap otherwise.

6.2 Expanding Generalization of Gödel's Spacetime

Plaue, Scherfner, and de Sousa Jr. (2008) present a way of constructing spacetimes with given kinematical invariants. As an example of their technique, the authors give a generalization of the Gödel spacetime that exhibits expansion. The line element reads

$$ds^2 = dt^2 - S^2(t) dx^2 + \frac{1}{2}e^{2\sqrt{2}x} (2 - S^2(t)) dy^2 - S^2(t) dz^2 + 2e^{\sqrt{2}x} dt dy, \quad (6.4)$$

where $S(t)$ is called scale parameter and obeys

$$\theta(t) = 3 \frac{\dot{S}(t)}{S(t)},$$

along with another differential equation; $\theta(t)$ is the expansion. For our purposes, it is sufficient to consider $S(t) = \exp(1/3 \theta(t) t)$.

Figure 6.8 shows six sets of geodesics with identical initial conditions but in spacetimes with different values for the expansion θ . Without expansion, the structure is reminiscent of what happens in the original Gödel spacetime: the geodesics form a caustic and refocus. With growing θ , however, the refocusing is increasingly dissolved.

Plaue, Scherfner, and de Sousa Jr. (2008) also develop a criterion for the absence of closed timelike or lightlike curves. It says that there can be no closed timelike or lightlike curves wherever the spatial part of the metric is negative definite. In the case of (6.4), this means that the spacetime is causal where $S^2(t) > 2$. The area above the surface $S^2(t) = 2$ is thus free of closed timelike or lightlike curves. This is exemplarily shown by the behavior of the light cones shown in figure 6.9. Below the surface, they exhibit the characteristic tipping for large x values that makes closed timelike curves possible. When we move upwards towards the surface however, the light cones tilt back, up to the point of being upright above the surface.

6.3 Ori's Time-Machine Spacetimes

Amos Ori has been publishing multiple spacetimes that resemble “time machines” in so far as they allow closed timelike or lightlike curves only in confined regions which are, furthermore, controllable in some sense. Ori also strives to find well-defined matter models for his spacetimes so that they satisfy the various energy conditions.

Ori (1993) presents the first such spacetime as a perturbation of the Minkowski spacetime in cylindrical coordinates:

$$\begin{aligned} ds^2 &= dt^2 - dr^2 - r^2 d\phi^2 - dz^2 - d\tilde{s}^2, \\ d\tilde{s}^2 &= 2r h(\rho) \left(a t dt - b((r - r_0)dr + z dz) \right) d\phi + r^2 h^2(\rho) (b^2 \rho^2 - a^2 t^2) d\phi^2, \end{aligned}$$

where $a, b, r_0 > 0$ and $0 < d < r_0$ are parameters² and $\rho^2 := (r - r_0)^2 + z^2$. The surfaces $\rho = \text{const}$ define tori. The scale factor $h(\rho)$ confines the perturbation to the interior of a

²For the figures, we choose $r_0 = 3$, $d = 1$, $a = 6/d$, and $b = 2/d$.

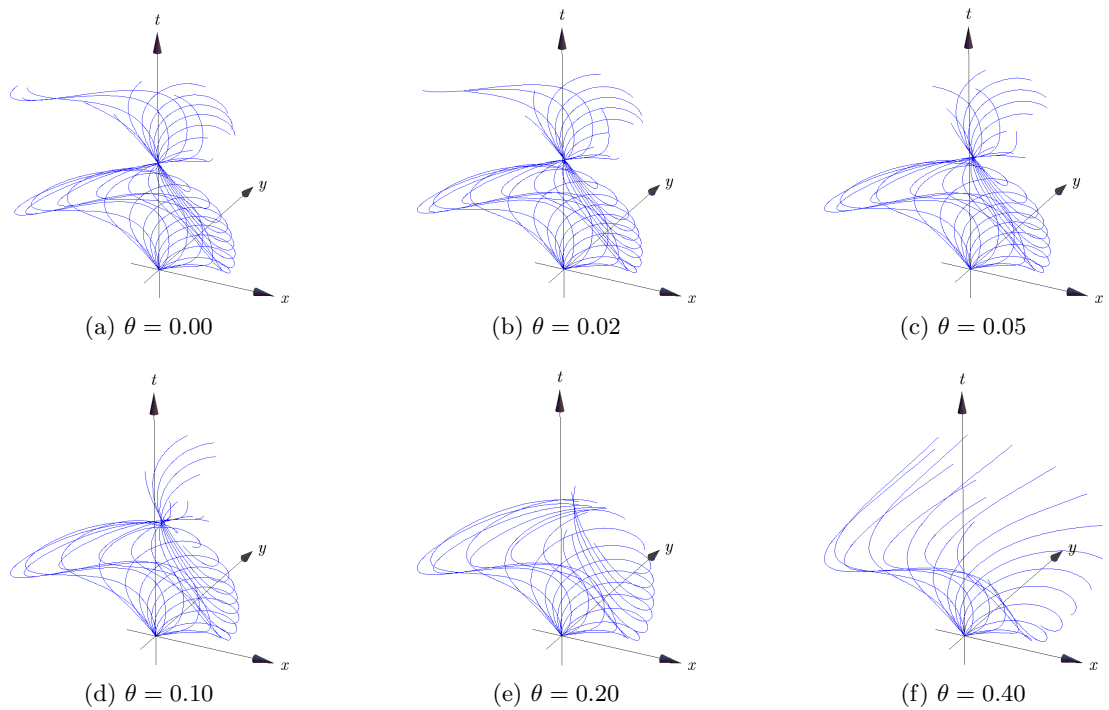


Figure 6.8: Six sets of geodesics with the same initial conditions but with different values for the expansion θ . As the expansion grows, the geodesics' refocusing increasingly dissolves.

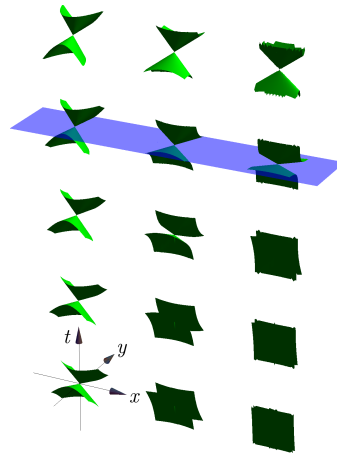


Figure 6.9: Causality change in the expanding generalization of Gödel's spacetime. The blue surface marks the border above which no closed timelike curves can exist. The characteristic tipping of the light cones below the surface is continually reversed when nearing the surface. Above the surface, the light cones are upright.

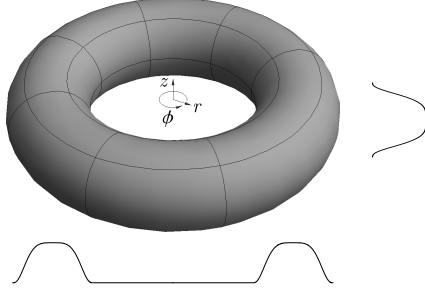


Figure 6.10: The torus outside of which the scale factor $h(\rho)$ vanishes and where the metric is thus equal to the Minkowski metric. Below and to the right of the torus the r and the z profile of $h(\rho)$ are shown.

spatial torus of finite size:

$$h(\rho) := \begin{cases} (1 - (\rho/d)^4)^3 & \text{if } \rho < d, \\ 0 & \text{otherwise.} \end{cases}$$

The torus $h(\rho) = d$ is shown in figure 6.10, along with the r and z profiles of h .

Inside this torus, the perturbation causes the light cones to tip over increasingly when moving to larger t values. This is demonstrated in figure 6.11 which shows the same situation for three different t values. In contrast to the previous figure, the coordinates (r, ϕ, t) are now used instead of (r, ϕ, z) . So the torus is now indicated by two cylinders. For all three t values, the light cones are upright outside the torus since the metric is that of Minkowski spacetime there. Inside the torus, however, the perturbation changes the metric in such a way that the light cones start to tip over for $t > 0$. At $t = 1/a$, the closed curve $\rho = 0$ is lightlike, and for $t > 1/a$ it is timelike.

Ori (1994) explains the spacetime in more detail, and Soen and Ori (1996) present a modification which satisfies more energy conditions.

Later, Ori (2005) presented an improved time-machine spacetime which develops closed timelike curves inside a vacuum core part surrounded by a matter field. We focus here on the vacuum core. The line element reads

$$ds^2 = 2dz dt - dx^2 - dy^2 - (e\rho^2 - t)dz^2 - 2((2e - a)x dx + (2e + a)y dy)dz. \quad (6.5)$$

With $\rho^2 = x^2 + y^2$ and $e, a > 0$. The coordinate z is periodic, $z \in [0, L]$ for some $L > 0$, and $z = 0$ and $z = L$ are identified. The other coordinates take all real values. Thus, the spacetime has the somewhat unusual topology of $\mathbb{R}^3 \times S^1$.

We choose e and a such that $e > (2e + a)^2$. Then we have

$$\begin{aligned} g^{tt} &= e\rho^2 - t - (2e - a)^2 x^2 - (2e + a)^2 y^2 \\ &> e\rho^2 - t - (2e + a)^2 x^2 - (2e + a)^2 y^2 \\ &> -t. \end{aligned}$$

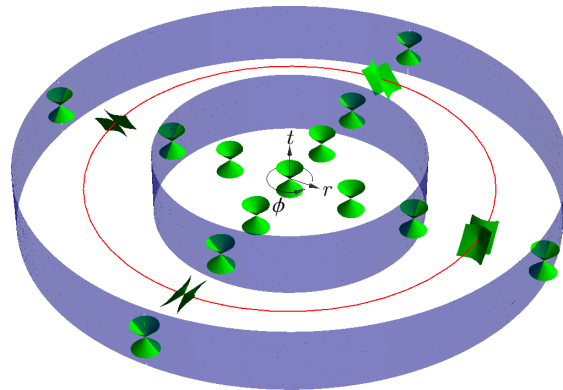
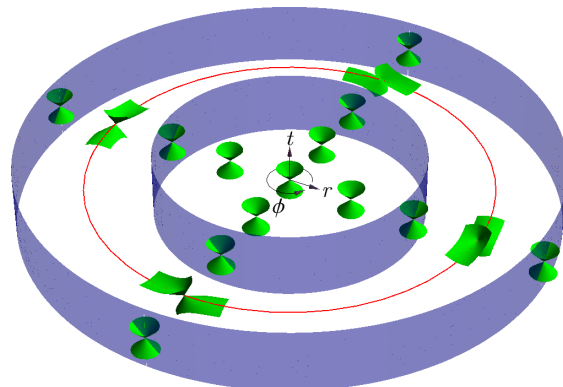
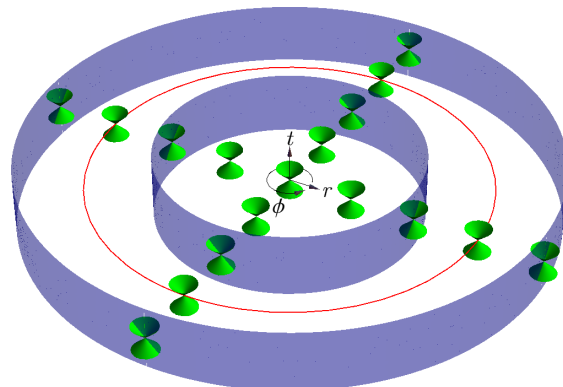
(a) $t = 2/a$ (b) $t = 1/a$ (c) $t = 0$

Figure 6.11: The same set of light cones for different t values. Inside the torus, here shown as two cylinders, the light cones start to tip over for $t > 0$. At $t = 1/a$, the closed curve $\rho = 0$, shown in red, is lightlike, and for $t > 1/a$ it is timelike.

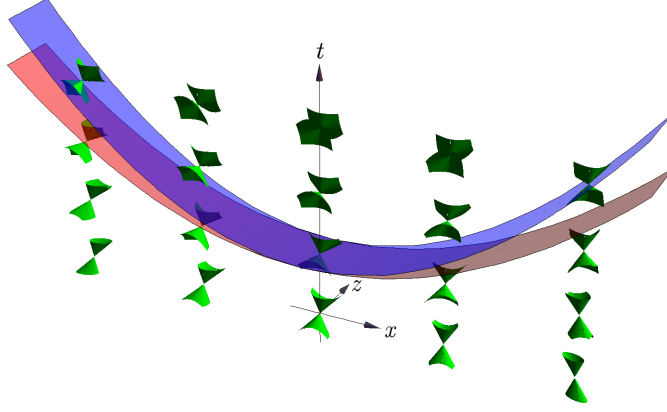


Figure 6.12: Behavior of light cones in Ori's time-machine spacetime (6.5). The coordinate y is suppressed, and $e = 1/8$ and $a = 1/16$ are used. The dark contour marks the causality border of the hypersurfaces $t = \text{const}$. Similarly, the lighter contour marks the causality border for the directions ∂_z .

So the hypersurfaces $t = \text{const}$ are spacelike at $t < 0$. For $t \geq 0$, the hypersurfaces are mixed: causal for small ρ and spacelike for large ρ . And since $g_{zz} = t - e\rho^2$, the closed curves ∂_z are timelike at $t > e\rho^2$. This region lies completely inside the region where $t = \text{const}$ is causal. The light cones behave accordingly: for growing t , they open up so that $t = \text{const}$ becomes causal, and they also tip over so that ∂_z becomes causal. These observations are depicted in figure 6.12, where the coordinate y is suppressed. It should be stressed that the existence of closed timelike curves in this spacetime appears to depend crucially on its unusual topology.

Interestingly, the criterion for the spacelikeness of the hypersurfaces $t = \text{const}$ matches a criterion for the absence of closed timelike or null curves developed by Plaue, Scherfner, and de Sousa Jr. (2008) and described in section 6.2. It says that there can be no closed timelike or null curves wherever the spatial part of the metric is negative definite. The determinant of the spatial part of Ori's core metric turns out to be $-g^{tt}$, however. So this criterion says that there cannot be any closed timelike or null curves wherever $g^{tt} > 0$, which is exactly where the hypersurfaces $t = \text{const}$ are spacelike.

Very recently, Ori (2007) presented a spacetime made up of three parts fit together: a vacuum core, a dust shell, and a vacuum exterior. Inside the vacuum core, closed timelike curves develop. The metric of the vacuum core arises from the Schwarzschild metric (3.2) by a Wick rotation $\theta \rightarrow i\theta$ followed by a transformation akin to but different from the usual Eddington-Finkelstein transformation:

$$t \rightarrow v, \quad v = -(t + r^*), \quad r^* = r + 2\mu \ln \left(\frac{r}{2\mu} - 1 \right). \quad (6.6)$$

The result is

$$ds^2 = \left(1 - \frac{2\mu}{r} \right) dv^2 + 2dvdr + r^2 (d\theta^2 + \sinh^2 \theta d\phi^2).$$

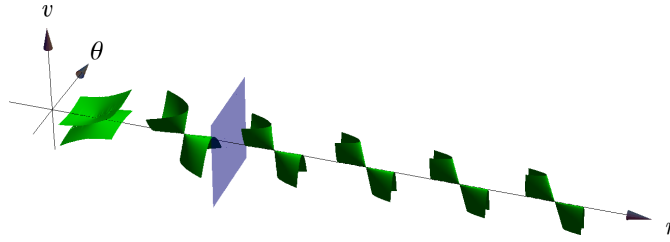


Figure 6.13

The coordinates have the usual ranges except for v which is defined to be periodic on $[0, L]$. Similarly to the previous spacetime, this enforces the topology $S^1 \times \mathbb{R}^3$. In the region $r < 2\mu$, the light cones tip over in such a way that the closed curves ∂_v become timelike. This is depicted in figure 6.13.

Bibliography

- Andréka, H. et al. (2008). *Visualizing some ideas about Gödel-type rotating universes*. arXiv: 0811.2910.
- Beem, J. K., P. E. Ehrlich, and K. L. Easley (1996). *Global Lorentzian Geometry*. 2nd ed. Pure and Applied Mathematics. CRC Press.
- Bell, J. L. (2002). “Time and Causation in Gödel’s Universe”. In: *Transcendent Philosophy* 3.4.
- Bryson, S. (1992). “Virtual spacetime: an environment for the visualization of curved spacetimes via geodesic flows”. In: *VIS '92: Proceedings of the 3rd conference on Visualization '92*. Los Alamitos, CA, USA: IEEE Computer Society Press, pp. 291–298. ISBN: 0-8186-2896-0.
- Carlbom, I. and J. Paciorek (1978). “Planar Geometric Projections and Viewing Transformations”. In: *ACM Computing Surveys* 10.4, p. 465. DOI: 10.1145/356744.356750.
- Carter, B. (1966). “Complete Analytic Extension of the Symmetry Axis of Kerr’s Solution of Einstein’s Equations”. In: *Physical Review* 141.4, p. 1242. DOI: 10.1103/PhysRev.141.1242.
- Chandrasekhar, S. and J. P. Wright (1961). “The Geodesics in Gödel’s Universe”. In: *Proceedings of the National Academy of Science* 47, pp. 341–347.
- Davidson, A. (2000). “Extensible Embeddings of Black-Hole Geometries”. In: *Foundations of Physics* 30.5, p. 785. DOI: 10.1023/A:1003793128801.
- Fox, L. and D. F. Mayers (1988). *Numerical Solution of Ordinary Differential Equations*. Chapman & Hall. ISBN: 0412226502.
- Frolov, V. P. (2006). “Embedding of the Kerr-Newman black hole surface in Euclidean space”. In: *Physical Review D* 73.6, p. 064021. DOI: 10.1103/PhysRevD.73.064021.
- Gallot, S., D. Hulin, and J. Lafontaine (2004). *Riemannian Geometry*. 3rd ed. Universitext. Springer.
- Giblin, J. T. (2004). “Space–time slices and surfaces of revolution”. In: *Journal of Mathematical Physics* 45.12, p. 4551. DOI: 10.1063/1.1808487.
- Giblin, J. T., D. Marolf, and R. H. Garvey (2004). “Spacetime Embedding Diagrams for Spherically Symmetric Black Holes”. In: *General Relativity and Gravitation* 36, p. 83. arXiv: gr-qc/0305102v2.
- Gödel, K. (1949). “An Example of a New Type of Cosmological Solutions of Einstein’s Field Equations of Gravitation”. In: *Reviews of Modern Physics* 21.3, p. 447. DOI: 10.1103/RevModPhys.21.447.
- Hawking, S. W. and G. F. R. Ellis (1973). *The Large Scale Structure of Space-Time*. Cambridge Monographs on Mathematical Physics. Cambridge University Press.

- Hitchin, N. (2003). *Differentiable Manifolds*. Lecture notes from the University of Oxford. URL: <http://people.maths.ox.ac.uk/~hitchin/hitchinnotes/hitchinnotes.html>.
- Hledík, S. (2001). “Embedding diagrams of the ordinary and optical reference geometry of black-hole spacetimes and their astrophysical relevance”. In: *RAGtime 2/3: Workshops on Black Holes and Neutron Stars*. Ed. by S. Hledík and Z. Stuchlík, pp. 25–52.
- Jänich, K. (2005). *Vektoranalysis*. 5th ed. Springer-Lehrbuch. Springer Berlin Heidelberg.
- Jonsson, R. M. (2001). “Embedding spacetime via a geodesically equivalent metric of Euclidean signature”. In: *General Relativity and Gravitation* 33, p. 1207. DOI: 10.1023/A:1012037418513. arXiv: 0708.2381v1.
- (2005). “Visualizing curved spacetime”. In: *American Journal of Physics* 73.3, p. 248. DOI: 10.1119/1.1830500.
- Kristiansson, S. (1998). “Optical Space of the Reissner-Nordström Solutions”. In: *General Relativity and Gravitation* 30.2, p. 275. DOI: 10.1023/A:1018800912591.
- Kundt, W. (1956). “Trägheitsbahnen in einem von Gödel angegebenen kosmologischen Modell”. In: *Zeitschrift für Physik* 145.5, p. 611. DOI: 10.1007/BF01332282.
- Lovelock, D. and H. Rund (1975). *Tensors, Differential Forms, and Variational Principles*. Wiley.
- Malament, D. B. (1984). ““Time Travel” in the Gödel Universe”. In: *PSA: Proceedings of the Biennial Meeting of the Philosophy of Science Association* 2, pp. 91–100.
- Marolf, D. (1999). “Spacetime Embedding Diagrams for Black Holes”. In: *General Relativity and Gravitation* 31.6, p. 919. DOI: 10.1023/A:1026646507201.
- Misner, C. W., K. S. Thorne, and J. A. Wheeler (1973). *Gravitation*. W. H. Freeman. ISBN: 0-7167-0344-0.
- O’Neill, B. (1983). *Semi-Riemannian geometry*. Academic Press, New York. ISBN: 0125267401.
- Ori, A. (1993). “Must time-machine construction violate the weak energy condition?” In: *Physical Review Letters* 71.16, p. 2517. DOI: 10.1103/PhysRevLett.71.2517.
- (1994). “Causality violation and the weak energy condition”. In: *Physical Review D* 49.8, p. 3990. DOI: 10.1103/PhysRevD.49.3990.
- (2005). “A Class of Time-Machine Solutions with a Compact Vacuum Core”. In: *Physical Review Letters* 95.2, p. 021101. DOI: 10.1103/PhysRevLett.95.021101.
- (2007). “Formation of closed timelike curves in a composite vacuum/dust asymptotically flat spacetime”. In: *Physical Review D* 76.4, p. 044002. DOI: 10.1103/PhysRevD.76.044002.
- Pfarr, J. (1981). “Time travel in Gödel’s space”. In: *General Relativity and Gravitation* 13.11, p. 1073. DOI: 10.1007/BF00756366.
- Pinkall, U. and P. Peters (2006/2007). *Differentialgeometrie II*. Lecture notes from the TU Berlin.
- Plaue, M., M. Scherfner, and L. A. M. de Sousa Jr. (2008). *On Spacetimes with Given Kinematical Invariants: Construction and Examples*. arXiv: 0801.3364v2.
- Romano, J. D. (1995). “Embedding initial data for black-hole collisions”. In: *Classical and Quantum Gravity* 12.3, p. 875. DOI: 10.1088/0264-9381/12/3/023.

- Rosa, V. M. and P. S. Letelier (2007). *Stability of Closed Timelike Curves in Goedel Universe*. arXiv: [gr-qc/0703100v2](https://arxiv.org/abs/gr-qc/0703100v2).
- Rosen, N. (1985). “Some Schwarzschild solutions and their singularities”. In: *Foundations of Physics* 15.4, pp. 517–529. DOI: [10.1007/BF01889285](https://doi.org/10.1007/BF01889285).
- Sachs, R. K. and H. H. Wu (1977). *General Relativity for Mathematicians*. Graduate Texts in Mathematics. Springer. ISBN: 038790218X.
- Sahdev, D., R. Sundararaman, and M. S. Modgil (2006). *The Gödel Universe: A Practical Travel Guide*. arXiv: [gr-qc/0611093v1](https://arxiv.org/abs/gr-qc/0611093v1).
- Soen, Y. and A. Ori (1996). “Improved time-machine model”. In: *Physical Review D* 54.8, p. 4858. DOI: [10.1103/PhysRevD.54.4858](https://doi.org/10.1103/PhysRevD.54.4858).
- Stein, H. (1970). “On the Paradoxical Time-Structures of Gödel”. In: *Philosophy of Science* 37.4, pp. 589–601.
- Von Borzeszkowski, H.-H. and T. Chrobok (2005/2006). *Allgemeine Relativitätstheorie I + II*. Lecture notes from the TU Berlin.